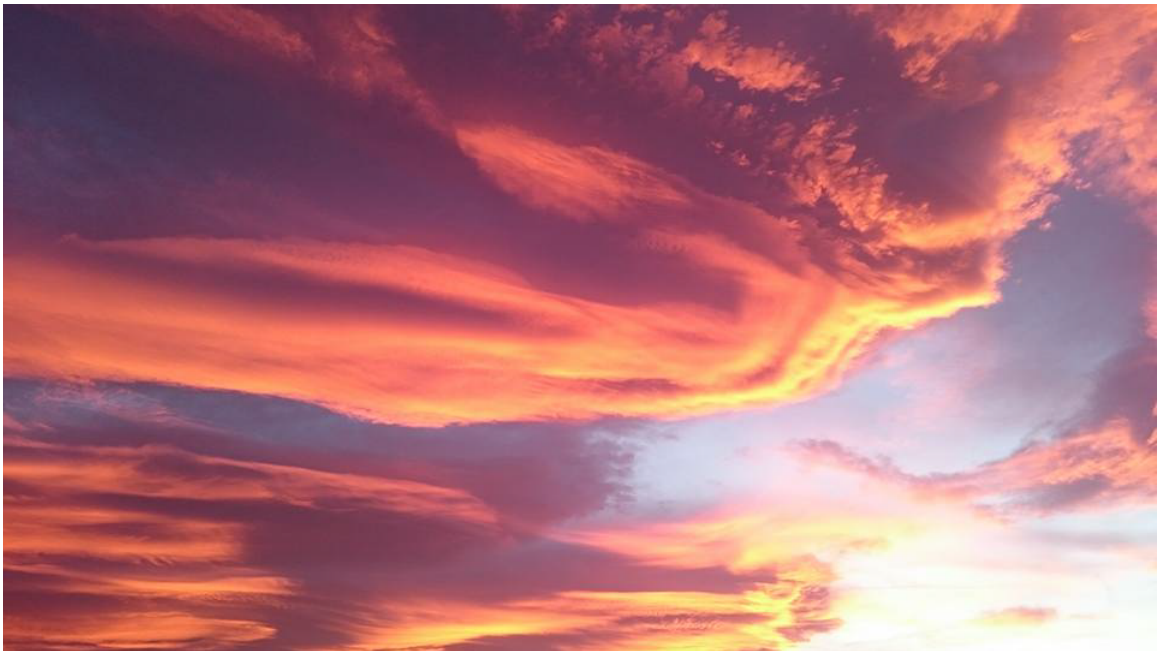




Linking spring North Atlantic sea surface
temperature anomalies to the occurrence of
European summer heatwaves



Goratz Beobide Arsuaga

Hamburg 2023

Hinweis

Die Berichte zur Erdsystemforschung werden vom Max-Planck-Institut für Meteorologie in Hamburg in unregelmäßiger Abfolge herausgegeben.

Sie enthalten wissenschaftliche und technische Beiträge, inklusive Dissertationen.

Die Beiträge geben nicht notwendigerweise die Auffassung des Instituts wieder.

Die "Berichte zur Erdsystemforschung" führen die vorherigen Reihen "Reports" und "Examensarbeiten" weiter.

Anschrift / Address

Max-Planck-Institut für Meteorologie
Bundesstrasse 53
20146 Hamburg
Deutschland

Tel./Phone: +49 (0)40 4 11 73 - 0
Fax: +49 (0)40 4 11 73 - 298

name.surname@mpimet.mpg.de
www.mpimet.mpg.de

Notice

The Reports on Earth System Science are published by the Max Planck Institute for Meteorology in Hamburg. They appear in irregular intervals.

They contain scientific and technical contributions, including PhD theses.

The Reports do not necessarily reflect the opinion of the Institute.

The "Reports on Earth System Science" continue the former "Reports" and "Examensarbeiten" of the Max Planck Institute.

Layout

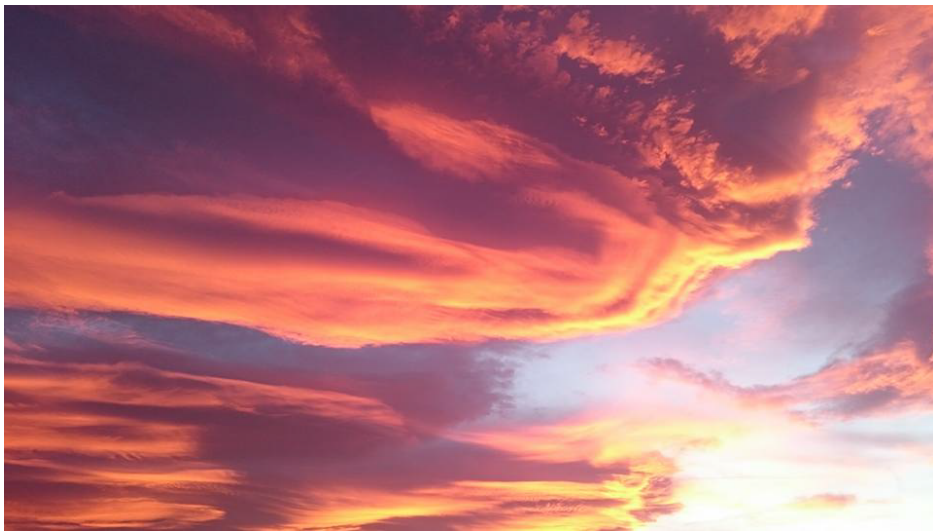
*Bettina Diallo and Norbert P. Noreiks
Communication*

Copyright

*Photos below: ©MPI-M
Photos on the back from left to right:
Christian Klepp, Jochem Marotzke,
Christian Klepp, Clotilde Dubois,
Christian Klepp, Katsumasa Tanaka*



Linking spring North Atlantic sea surface
temperature anomalies to the occurrence of
European summer heatwaves



Goratz Beobide Arsuaga

Hamburg 2023

Goratz Beobide Arsuaga

aus Zarautz, Spanien

Max-Planck-Institut für Meteorologie
The International Max Planck Research School on Earth System Modelling
(IMPRS-ESM)
Bundesstrasse 53
20146 Hamburg

Universität Hamburg
Fachbereich Erdsystemwissenschaften
Institut für Meereskunde
Bundesstraße 53
20146 Hamburg

Tag der Disputation: 27. September 2023

Folgende Gutachter empfehlen die Annahme der Dissertation:

Prof. Dr. Johanna Baehr
Dr. Wolfgang A. Müller

Vorsitzender des Promotionsausschusses:

Prof. Dr. Hermann Held

Dekan der MIN-Fakultät:

Prof. Dr.-Ing. Norbert Ritter

The front cover photo was taken by the author in Zarautz during an episode of extreme heat. This document was typeset using the `classicthesis` template developed by André Miede and Ivo Pletikosić available at: <https://bitbucket.org/amiede/classicthesis/>.

ABSTRACT

The frequency and intensity of European summer heatwaves (EuSHWs) have increased in recent years causing large humanitarian and economic losses. Yet, our ability to anticipate the occurrence of EuSHWs is very limited, and the timing and location of EuSHWs can only be predicted a week in advance. Several case studies suggested that North Atlantic sea surface temperature anomalies (SSTAs) might precede EuSHWs, indicating different patterns as early as in spring. Such SSTAs might have influenced the occurrence of past EuSHWs. However, the limited number of observed events associated with several physical mechanisms prevented a robust identification of spring North Atlantic SSTAs as precursors of different EuSHWs. In this dissertation, I identify the most important spring North Atlantic SSTAs that precede EuSHWs to, in turn, open the possibility of extending the predictability of EuSHWs up to a season ahead.

I overcome the limitation of case studies by combining 100 historical simulations of the MPI Grand-Ensemble with explainable neural networks. I find that a spring North Atlantic tripolar pattern with positive SSTAs in the Subtropical Gyre is a common precursor of EuSHWs. The North Atlantic tripolar pattern with positive SSTAs in the Subtropical Gyre is related to negative winter and spring precipitation anomalies over Europe, which reduce the soil moisture and precondition the occurrence of EuSHWs. Furthermore, I find that positive spring SSTAs in distinct regional seas are a precursor of distinct EuSHWs. While positive SSTAs around the Iberian Peninsula indicate the occurrence of western EuSHWs, positive SSTAs in the Mediterranean, North, and Baltic Seas indicate the occurrence of southeastern EuSHWs. Positive regional SSTAs enhance the persistence of spring high-pressure anomalies in different parts of Europe, reducing the precipitation and early summer soil moisture, and preconditioning the occurrence of distinct EuSHWs.

However, a relatively coarse resolution of the MPI-Grand Ensemble leads to model biases, and the model might misrepresent the relationships between spring North Atlantic SSTAs and EuSHWs. Therefore, I test the applicability of the spring North Atlantic tripolar pattern and regional SSTAs to anticipate the occurrence of recent EuSHWs. I employ the GFCS2.1 seasonal forecast system initialized in May, which runs the high-resolution version of the MPI-ESM model, as well as ERA5 reanalysis product, and EOBS and OISST observational datasets. I find that in all datasets the probability of western EuSHW occurrence is increased with the spring tripolar North Atlantic pattern with positive SSTAs in the Subtropical Gyre, and with positive SSTAs around the Iberian Peninsula. Furthermore, the probability of southeastern EuSHW occurrence is increased with positive spring SSTAs in the Mediterranean, North, and Baltic Seas. In contrast, the probability of EuSHW occurrence is reduced with negative spring SSTAs averaged over the regional seas.

Overall, this dissertation contributes towards the seasonal predictability of EuSHWs and it opens an opportunity to develop an early warning system of EuSHWs based on spring North Atlantic SSTAs.

ZUSAMMENFASSUNG

Die Häufigkeit und Intensität der sommerlichen Hitzewellen in Europa (EuSHW) haben in den letzten Jahren zugenommen und verursachen große humanitäre und wirtschaftliche Verluste. Dennoch ist unsere Möglichkeit, das Auftreten von EuSHWs vorherzusehen, sehr begrenzt, und der Zeitpunkt und der Ort von EuSHWs können nur eine Woche im Voraus vorhergesagt werden. Mehrere Fallstudien deuten darauf hin, dass Anomalien der Meeresoberflächentemperatur (SSTAs) des Nordatlantiks den EuSHWs vorausgehen könnten und bereits im Frühjahr unterschiedliche Muster aufweisen. Solche SSTAs könnten das Auftreten vergangener EuSHWs beeinflusst haben. Die begrenzte Zahl der beobachteten Ereignisse, die mit verschiedenen physikalischen Mechanismen in Verbindung gebracht werden, verhinderte jedoch eine eindeutige Identifizierung der nordatlantischen Frühjahrs-SSTAs als Vorläufer verschiedener EuSHWs. In dieser Dissertation identifiziere ich die wichtigsten nordatlantischen Frühjahrs-SSTAs, die EuSHWs vorausgehen und eröffne damit die Möglichkeit, die Vorhersagbarkeit von EuSHWs auf eine Saison im Voraus zu erweitern.

Ich bewältige die Einschränkungen von Fallstudien, indem ich 100 historische Simulationen des MPI Grand-Ensemble mit erklärbaren neuronalen Netzen kombiniere. Ich stelle fest, dass ein tripolares Frühjahrs muster im Nordatlantik mit positiven SSTAs im Subtropischen Wirbel ein häufiger Vorläufer von EuSHWs ist. Das nordatlantische tripolare Muster mit positiven SSTAs im Subtropischen Wirbel steht im Zusammenhang mit negativen Winter- und Frühlingsniederschlagsanomalien über Europa, die die Bodenfeuchtigkeit verringern und das Auftreten von EuSHWs voraussetzen. Darüber hinaus stelle ich fest, dass positive Frühjahrs-SSTAs in verschiedenen regionalen Meeren ein Vorläufer für verschiedene EuSHWs sind. Während positive SSTAs um die Iberische Halbinsel auf das Auftreten westlicher EuSHWs hinweisen, deuten positive SSTAs im Mittelmeer, der Nord- und Ostsee auf das Auftreten südöstlicher EuSHWs hin. Positive regionale SSTAs verstärken die Persistenz von Frühjahrs-Hochdruckanomalien in verschiedenen Teilen Europas, verringern die Niederschläge und die Bodenfeuchtigkeit im Frühsommer und sind die Voraussetzung für das Auftreten von ausgeprägten EuSHWs.

Die relativ grobe Auflösung des MPI-Grand Ensemble führt jedoch zu Modellverzerrungen und das Modell könnte die Beziehungen zwischen den SSTAs im Frühjahr im Nordatlantik und den EuSHWs falsch darstellen. Daher prüfe ich die Anwendbarkeit des tripolaren Frühjahrs musters des Nordatlantiks und der regionalen SSTAs zur Vorhersage des Auftretens der jüngsten EuSHWs. Ich verwende das saisonale Vorhersagesystem GFCS2.1, das im Mai initialisiert wurde und mit der hochauflösenden Version des MPI-ESM-Modells sowie mit dem Reanalyseprodukt ERA5 und den Beobachtungsdatensätzen EOBS und OISST arbeitet. Ich stelle fest, dass in allen Datensätzen die Wahrscheinlichkeit des Auftretens des westlichen EuSHW mit dem tripolaren nordatlantischen Frühjahrs muster mit positiven SSTAs im Subtropischen Wirbel und mit positiven SSTAs um die Iberische Halbinsel erhöht ist. Darüber hinaus wird die Wahrscheinlichkeit des Auftretens von EuSHW im Südosten durch positive Frühjahrs-SSTAs im Mittelmeer, in der Nord-

und Ostsee erhöht. Im Gegensatz dazu verringert sich die Wahrscheinlichkeit des Auftretens von EuSHW bei negativen Frühjahrs-SSTAs im Durchschnitt über die regionalen Meere.

Insgesamt leistet diese Dissertation einen Beitrag zur saisonalen Vorhersagbarkeit von EuSHWs und eröffnet eine Möglichkeit, ein Frühwarnsystem für EuSHWs auf der Grundlage der nordatlantischen Frühjahrs-SSTAs, zu entwickeln.

PUBLICATIONS RELATED TO THIS DISSERTATION

Appendix A:

Beobide-Arsuaga, G. (2023). "European summer heatwave catalogue". DOKU at DKRZ. https://www.wdc-climate.de/ui/entry?acronym=DKRZ_LTA_1075_ds00028.

Appendix B

Beobide-Arsuaga, G., Düsterhus, A., Müller, W. A., Barnes, E. A., and Baehr, J. (2023). "Spring Regional Sea Surface Temperatures as a Precursor of European Summer Heatwaves". *Geophysical Research Letters*, 50(2), e2022GL100727, <https://doi.org/10.1029/2022GL100727>.

Appendix C

Beobide-Arsuaga, G., Düsterhus, A., Müller, W. A., and Baehr, J. (2023). "On the applicability of spring North Atlantic sea surface temperatures as an indicator of European summer heatwaves" - *to be submitted*.

ACKNOWLEDGMENTS

The completion of this three-and-a-half-year-long journey would have not been possible without the guidance, support, and company of so many people.

My enormous gratitude to my supervisors André Düsterhus, Wolfgang A. Müller, and Johanna Baehr for their guidance. Thank you, André, for the insightful discussions on statistics and for being available anytime I needed help. Even though we only managed to see each other once in person, I never felt we were a sea away. Thank you, Wolfgang, for welcoming my unexpected visits to your office and the interesting discussions on the North Atlantic air-sea interactions. And especially, thank you, Johanna, for everything. Thank you for being such an amazing supervisor and mentor. You were always ready to help in the most difficult times, no matter if the issue was concerning my Ph.D. project or my personal life. I am so grateful for having the opportunity to work under your supervision and be part of your group.

Climate Modelling, what an inspiring group of people! I learned so much from all of you. I deeply enjoyed the group meetings, the spontaneous talks and coffees together, and the days we spent during the group retreats. Thanks, Björn, for your help when I started working with neural networks. You saved me from several frustrating days. Thanks, Sebastian, for making it easy to obtain all the data needed for my research. Thanks for the interesting conversations while having coffee outside the office, even on cold and windy winter days. I will miss the sound of your coffee grinder through the hallway. Thanks, Edu, for being such an excellent office mate. Thanks for being so patient and helpful during the last stressful months. Thank you, David, for your feedback on several manuscripts. I enjoyed so much the time we spent together inside and outside of work.

I would like to extend my gratitude to the IMPRS-ESM graduate school for creating such an excellent environment to grow as a scientist and pursue a Ph.D. degree. Thank you, Connie, Michaela, and specially Antje, for your help and support. I would also like to thank Francisca, who supported me from the very first day at work. A brief conversation with you is enough to feel all the positivism you transmit.

Last but not least, I would like to express my deepest appreciation to my family and life partners. Thanks to my family for their unconditional love and support. Thank you, Anna and Gota, for being my sunshine even in the darkest days.

CONTENTS

Unifying Essay	1
1 Introduction	3
1.1 How do European summer heatwaves form?	3
1.2 The influence of the North Atlantic Ocean	4
1.3 The power of MPI Grand-Ensemble, neural networks, and layerwise relevance propagation	6
2 Statistical definition and characterization of heatwaves	7
2.1 Defining heatwave days	8
2.2 Characterizing heatwaves	9
2.3 European summer heatwave catalogue	9
3 North Atlantic sea surface temperature anomalies as a precursor of European summer heatwaves: a climate model-based approach	10
4 On the applicability of spring North Atlantic sea surface temperature anomalies as an indicator of European summer heatwave occurrence	14
5 Conclusions and outlook	16
Appendices	19
A EUROPEAN SUMMER HEATWAVE CATALOGUE	21
1 Introduction	23
2 Data and Methods	23
2.1 Data	23
2.2 Methods	23
3 European summer heatwave catalogue	25
B SPRING REGIONAL SEA SURFACE TEMPERATURES AS A PRECURSOR OF EUROPEAN SUMMER HEATWAVES	29
1 Introduction	32
2 Data and Methods	33
2.1 Data	33
2.2 Identification and Quantification of Heatwaves	33
2.3 Neural-Network Set-Up	34
3 Results	35
4 Conclusions	38
5 Supplementary Information	40
C ON THE APPLICABILITY OF SPRING NORTH ATLANTIC SEA SURFACE TEMPERATURES AS AN INDICATOR OF EUROPEAN SUMMER HEATWAVES	43
1 Introduction	45
2 Data and Methods	46
3 Results	48
4 Discussion	52
5 Conclusions	53
BIBLIOGRAPHY	55

UNIFYING ESSAY

LINKING SPRING NORTH ATLANTIC SEA SURFACE TEMPERATURE ANOMALIES TO THE OCCURRENCE OF EUROPEAN SUMMER HEATWAVES

1 INTRODUCTION

Global mean surface temperatures have already increased by 1.1 °C since the pre-industrial times due to human activities according to the last report of the Intergovernmental Panel on Climate Change (IPCC, 2023). Albeit a one-degree increase might not create an immediate alarm in society, the increase in temperatures is not spatially and year-to-year uniform (Easterling et al., 1997; Meehl et al., 2012). Due to complex interactions between different components of the climate system, a small global long-term temperature change can result in a disproportional variability of the climate system leading to disastrous extreme events (Katz and Brown, 1992; Mearns et al., 1984).

Atmospheric heatwaves are one example of such extreme events. In recent decades the episodes of extreme heat have increased in frequency, duration, and intensity in almost every region of the world (Perkins-Kirkpatrick and Lewis, 2020). Europe in particular has been identified as a heatwave hotspot with increasing trends of up to four times larger than the rest of the northern mid-latitudes (Rousi et al., 2022). Recent European summer heatwaves (EuSHWs) led to devastating effects on human health, the energy sector, and agriculture (Añel et al., 2017; Brás et al., 2021; Lowe et al., 2011; Robine et al., 2008). Yet, the prediction of EuSHWs does not extend beyond one week (Lavaysse et al., 2019), which limits the preparedness and the potential to reduce the negative effects. This dissertation aims towards extending the predictability by identifying patterns in spring North Atlantic SSTAs related to the occurrence of EuSHWs.

1.1 *How do European summer heatwaves form?*

Heatwaves are meteorological events that are associated with anomalies in large-scale atmospheric circulation. Although EuSHWs can show different spatial patterns associated with different physical mechanisms, all of them have a common ingredient for their formation: persistent high-pressure anomalies over the affected area (Stefanon et al., 2012).

Three main physical processes relate the high-pressure systems to extreme mid-latitude temperatures in summer (Fig. 1) (Domeisen et al., 2023). First, high-pressure systems are characterized by a downward movement of the air (Treidl et al., 1981). The downward movement compresses and warms the air while reducing the relative humidity and restricting the formation of clouds. As a result, high-pressure systems provide a stable and cloudless atmosphere that allows further warming of the surface due to increased incoming solar radiation. Second, high-pressure systems block the westerly winds and restrict the intrusion of storms (Austin, 1980). In the case of persistent high-pressure systems land-atmospheric interactions start to

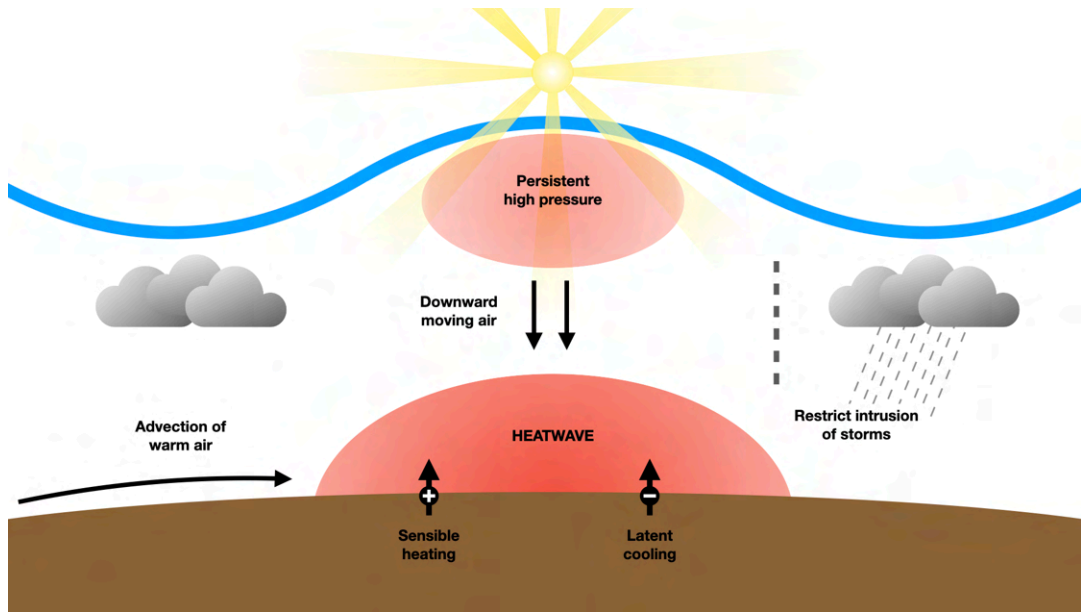


Figure 1: Schematic representation of the main physical processes that relate the high-pressure systems to mid-latitude summer heatwaves. Adapted from Domeisen et al. (2023).

play a role. The increased temperatures and reduced precipitation can desiccate the soil, reducing the latent cooling and increasing the sensible heating, and lead to an amplification of the intensity of heatwaves (Fischer et al., 2007; Seneviratne et al., 2006). Third, the circulation related to high-pressures advects warm southern air towards the north. The northward displacement of hot plumes is associated with the temperature peak of EuSHWs (Patterson, 2023).

Due to the chaotic behavior of the atmosphere, a successful prediction of persistent high-pressure systems and the consequent onset and location of EuSHWs does not extend beyond one week (Domeisen et al., 2023; Lavaysse et al., 2019). However, slowly varying North Atlantic sea surface temperatures are able to influence the atmospheric flow and precondition the occurrence of EuSHWs providing an opportunity to extend the predictability in several months (Domeisen et al., 2023; Gastineau and Frankignoul, 2015; Prodhomme et al., 2021).

1.2 The influence of the North Atlantic Ocean

The large-scale atmospheric and oceanic circulations over the North Atlantic are connected by the exchange of heat at interannual timescale (Bjerknes, 1964; Watanabe and Kimoto, 2000). It has been shown that a change in the large-scale atmospheric circulation affects North Atlantic sea surface temperatures, which persist over time and affects back the atmosphere creating positive feedback (Watanabe and Kimoto, 2000). The coupled large-scale patterns are the North Atlantic Oscillation in the atmosphere, a see-saw of surface pressures between the Azores high and the Icelandic low, and the North Atlantic tripolar pattern in the ocean, the SSTAs of opposite sign between the Subtropical Gyre, and the Subpolar Gyre and the tropical Atlantic (Bjerknes, 1964).

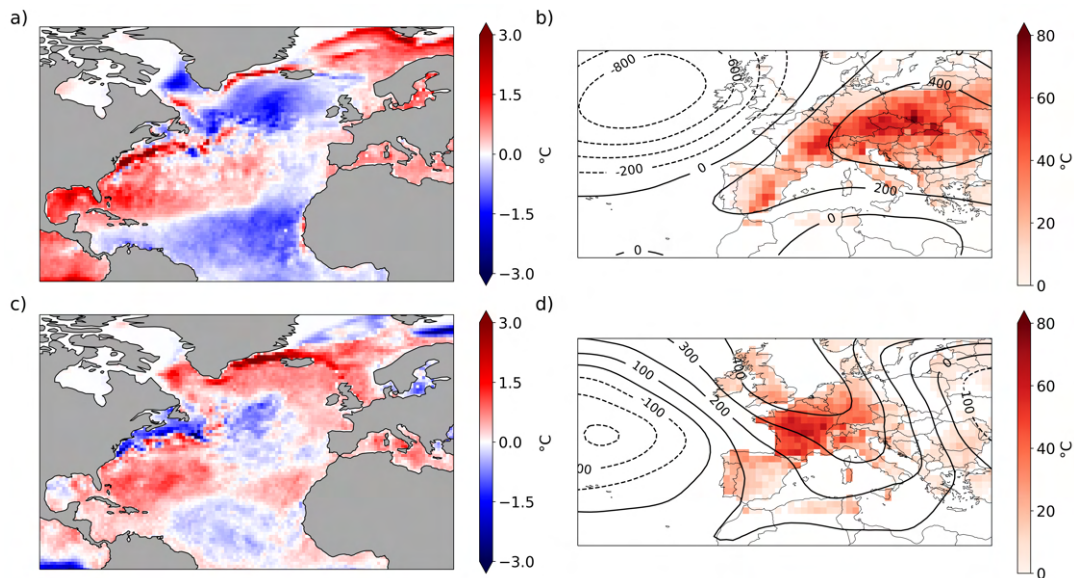


Figure 2: April and May mean sea surface temperature anomalies during the year: **(a)** 2015, **(c)** 2003. July and August 500hPa geopotential height anomalies in contour lines and the intensity of heatwaves expressed as cumulative heat in shading during the year: **(b)** 2015, **(d)** 2003.

The interaction between the atmosphere and the ocean over the North Atlantic also occurs at seasonal timescale. While the changes in the atmospheric circulation related to the winter North Atlantic Oscillation imprints the North Atlantic tripolar pattern, the tripolar pattern persists throughout spring and modulates the atmospheric flow (Chen et al., 2020; Czaja and Frankignoul, 1999, 2002; Song and Chen, 2023). Recent studies show that the spring North Atlantic tripolar pattern is related to high-pressure anomalies and precipitation anomalies over Europe (Gastineau and Frankignoul, 2015; Ossó et al., 2018; Song and Chen, 2023) which could precondition the occurrence of EuSHWs by reducing the soil moisture and triggering land-atmospheric interactions (Fischer et al., 2007; Seneviratne et al., 2006).

Several case studies suggested that the North Atlantic SSTAs influenced the occurrence of recent EuSHWs. On the one hand, the North Atlantic tripolar pattern has been related to the 2015 EuSHW (Fig. 2a,b) (Duchez et al., 2016; Wulff et al., 2017). According to Duchez et al. (2016), the negative SSTAs over the Subpolar Gyre were responsible for the displacement of the Jet Stream and the persistence of the high-pressure system over Europe leading to the occurrence of the 2015 EuSHW. In contrast, Wulff et al. (2017) proposed that tropical SSTAs and the respective diabatic forcing were responsible for the Rossby waves that perturbed the atmospheric flow and lead to the occurrence of the 2015 EuSHW.

On the other hand, SSTAs in different European regional seas have been related to the occurrence of the 2003 EuSHW (Fig. 2c,d) (Feudale and Shukla, 2007, 2011). Positive SSTAs in the North Sea reduced the meridional temperature gradient and the baroclinic activity enabling high-pressure to persist over Europe (Feudale and Shukla, 2011). The descending air associated to the high-pressure system restricted the formation of storms and increased the temperature of the Mediterranean Sea. Positive SSTAs in the Mediterranean Sea have been related to the reduction of Euro-

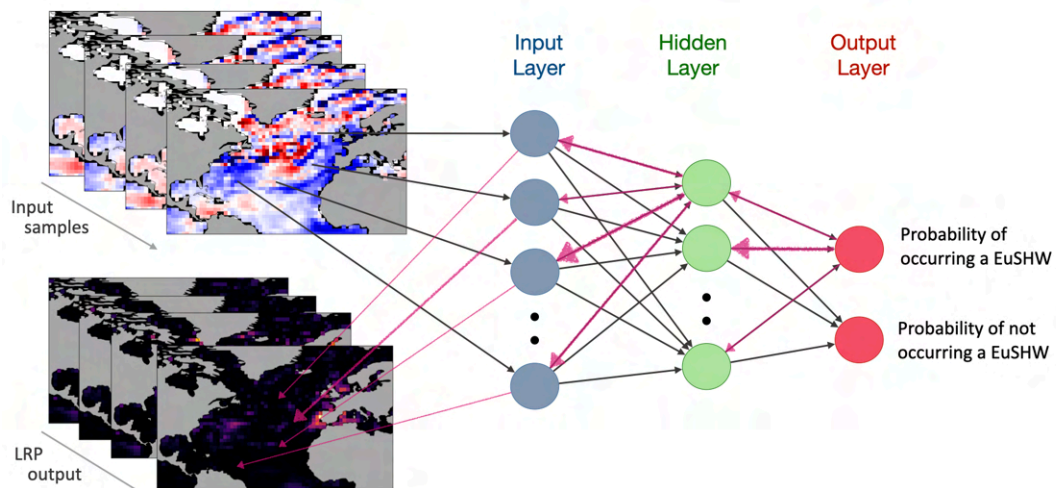


Figure 3: Illustration of a neural network model and the application of layerwise relevance propagation (LRP). The neural network model is designed to use April and May mean North Atlantic sea surface temperature anomalies (SSTAs) to provide the probability of European summer heatwave (EuSHW) occurrence. The arrows in black indicate the connection between neurons with weights and biases across three layers: the input layer (blue), the hidden layer (green), and the output layer (red). The arrows in magenta illustrate LRP, which provides the relevance of North Atlantic SSTAs to predict the probability of EuSHW occurrence. Adapted from Beobide-Arsuaga et al. (2023).

pean precipitation, and are considered responsible for half of the amplitude of the 2003 EuSHW (Feudale and Shukla, 2007; Ionita et al., 2017).

The 2003 and the 2015 EuSHWs illustrate the difficulty of generalizing from case studies the influence of spring North Atlantic SSTAs on the occurrence of EuSHWs. The low number of observed events that have been related to several physical processes impeded to robustly identifying the North Atlantic sea surface temperatures as a precursor of EuSHWs. Single model initial-condition large ensembles (SMILEs) combined with explainable neural networks offer a unique opportunity to robustly investigate the link between spring North Atlantic SSTAs and the occurrence of EuSHWs.

1.3 The power of MPI Grand-Ensemble, neural networks, and layerwise relevance propagation

SMILEs consist of a set of simulations based on a single climate model and exact natural and anthropogenic forcing but are started from different initial conditions (Maher et al., 2021). Due to the complex non-linear processes of the climate system, a small difference at the start of the simulation leads to very different weather and climate states (Lorenz, 1963). Hence, SMILEs provide different possible realizations of the climate system enabling a robust sampling of extreme events (Suarez-Gutierrez et al., 2018).

The MPI Grand-Ensemble is the largest ensemble of a single comprehensive climate model and contains 100 historical simulations spanning between 1850 and 2005 (Maher et al., 2019). The simulations are based on the low-resolution version of the MPI model and are forced with historical anthropogenic and natural emissions. In total, the historical MPI Grand-Ensemble offers 15,600 years to identify a large number of EuSHWs.

The historical MPI Grand-Ensemble simulations combined with neural networks, one of the most versatile machine learning methods able to capture complex non-linear relationships, provide a unique opportunity to relate spring North Atlantic SSTAs to the occurrence of EuSHWs (Dongare et al., 2012; Lecun et al., 2015). Neural networks consist of at least three consecutive layers of interconnected neurons with adjustable weights and biases (Fig. 3): the input layer where the model intakes information, one or several hidden layers where the information is non-linearly transformed by the activation function, and the output layer where the model provides the deduced result.

Neural networks have been successfully applied as a statistical prediction tool for different extreme climate events (Alemany et al., 2019; de Oliveira et al., 2009; Marzban and Witt, 2001). However, neural networks are often criticized for being “black boxes”: They might provide an accurate prediction but they lack interpretability on how they combine the input data across the weights and biases in order to deduce the result (Samek et al., 2021; Toms et al., 2020). The lack of interpretability has two main consequences. Firstly, the model might overfit the data and try to learn from noise. Secondly, the utility of neural networks is restricted to predicting a specific output and not to providing the mechanisms that lead to the prediction.

Layerwise relevance propagation, an explainable artificial intelligence method, aims to bring transparency into neural network models (Bach et al., 2015; Montavon et al., 2017; Toms et al., 2020). Layerwise relevance propagation provides the relevance of each input feature and sample for the outcome of the network (Fig. 3). The interpretability of neural networks not only increases the trust of neural networks as statistical prediction tools but also enables the discovery of new physical connections (Mayer and Barnes, 2021; Toms et al., 2021). In this dissertation, I combine the power of MPI Grand-Ensemble, neural networks, and layerwise relevance propagation to robustly identify the most relevant spring North Atlantic SSTAs to anticipate the occurrence of EuSHWs.

2 STATISTICAL DEFINITION AND CHARACTERIZATION OF HEATWAVES

The conceptual definition of heatwaves is relatively uniform among the literature, and it could be summarized as an unusual warming of the air, or intrusion of very warm air that affects a large area for several days to weeks (IPCC, 2021; WMO, 1992). However, the terms “warm air”, “large area” and “several days to weeks” are subjective, and it does not exist a universal definition for heatwaves. This brings us to the first challenge of this dissertation: The statistical identification and characterization of heatwaves.

2.1 *Defining heatwave days*

The statistical definition of heatwaves strongly depends on the purpose of the study. On the one hand, impact-based studies employ heatwave definitions with a specific targeted group in mind (e.g. human health, agriculture, transport, or energy sector), and can combine more than one variable to define a heatwave day (Barriopedro et al., 2023; Perkins and Alexander, 2013). Taking human health as an example, human comfort will not only depend on the daily maximum temperatures but also on the minimum temperatures reached at night, the humidity of the air, the wind speed, and the radiation (Błazejczyk et al., 2013). On the other hand, studies that focus on climate-related processes are usually based on univariate heatwave definitions, which generally use surface air temperatures (Barriopedro et al., 2023). In this dissertation, I use July and August daily maximum temperatures. The univariate heatwave indices, albeit being more straightforward than the multivariate ones, are not trivial. They require a selection of parameters and methodological choices that will lead to different results.

The most common climate-based heatwave definitions require defining a threshold that determines what an extreme is and defining the number of consecutive days that the threshold must be exceeded. The most simple approach is to define a fixed absolute value as a threshold (e.g. 30°C) and identify the days that rise above it over the desired number of consecutive days. However, the main drawback of fixed absolute thresholds is that they neglect the regional variations of the climate. The days that exceed the previous example of 30°C will be considerably larger in the Mediterranean regions when compared to the Scandinavian ones. A common approach to consider the regional differences is to apply a percentile-based threshold obtained from a distribution of each geographical point we aim to study during a reference period.

The percentile-based thresholds can also be of diverse complexity. The most simple form of a percentile-based threshold is computed from a single distribution of daily maximum temperatures. The largest constraint of the fixed percentile-based thresholds is that they do not consider the seasonal and long-term variability of the climate. A seasonally fixed threshold implies that heatwaves will be more likely to be identified during the climatological peak (i.e. at the end of July and the beginning of August in the mid-northern hemisphere; Fig. 4a). Similarly, an interannually fixed threshold implies that the identification of the heatwaves will be affected by the decadal variability of the climate and the long-term trend due to global warming (Fig. 4b). An alternative method is to apply a percentile-based threshold based on a seasonally and/or interannually varying distributions. While the seasonally-varying percentile-based heatwave definition accounts for the seasonality identifying a uniform number of heatwave days along calendar days (Fig. 4a), the interannually-varying percentile-based heatwave definition accounts for decadal variability and the long-term trend (Fig. 4b).

The selection of the percentile and the number of consecutive days that the threshold must be exceeded is to some extent arbitrary. Most of the studies use a range from the 80th to 95th percentile, and a range from three to six consecutive days (Della-Marta et al., 2007; Fischer and Schär, 2010; Stefanon et al., 2012; Vogel et al., 2020). The choice of the percentile number and the number of consecutive days

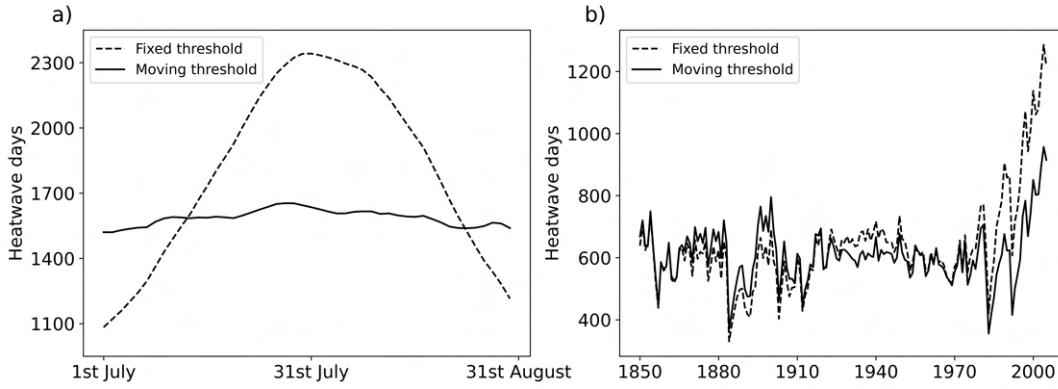


Figure 4: Number of identified heatwave days for historical (1850-2005) MPI Grand-Ensemble ensemble mean applying heatwave definitions with: (a) seasonally fixed and moving thresholds for each July and August calendar day; (b) interannually fixed and moving thresholds for each historical year. The seasonally moving threshold is based on a centered 15-day running window. The interannually moving threshold is based on a centered 31-year running window.

compromises the number of identified heatwave days and their intensity. While a higher percentile number and consecutive days lead to the identification of fewer but stronger heatwave days, a lower threshold and consecutive days lead to the identification of more but weaker heatwave days. In this dissertation, I use a time-varying percentile-based heatwave definition with 90th percentile and three consecutive days.

2.2 Characterizing heatwaves

Several metrics have been used in the literature to characterize heatwaves (Barriopedro et al., 2023). However, the most common metrics do not consider the multi-dimensional effects of heatwaves and only measure a single aspect of their characteristics: the intensity (e.g. maximum or averaged temperatures), the time (e.g. duration or frequency), or the space (e.g. spatial extent). A recent metric introduced by Perkins-Kirkpatrick and Lewis (2020), the cumulative heat, considers two of them: intensity and duration.

The cumulative heat represents the excess of heat contributed by heatwaves, and it is computed by a seasonal integration of daily maximum temperatures above the defined threshold during heatwave days (Fig. 5). This rather simple but informative metric also provides the option to combine the third dimension, the spatial dimension. By integrating the original cumulative heat metric over the area of interest, I obtain a single number per year that characterizes the intensity of EuSHWs.

2.3 European summer heatwave catalogue

Using ERA5 dataset for the period 1982-2022 and applying the seasonally-varying percentile-based heatwave definition combined with the cumulative heat metric I create a EuSHW catalogue (Beobide-Arsuaga (2023), Appendix A). The catalogue is part of my contribution to the ClimXtreme project (<https://climxtreme.net/index>.

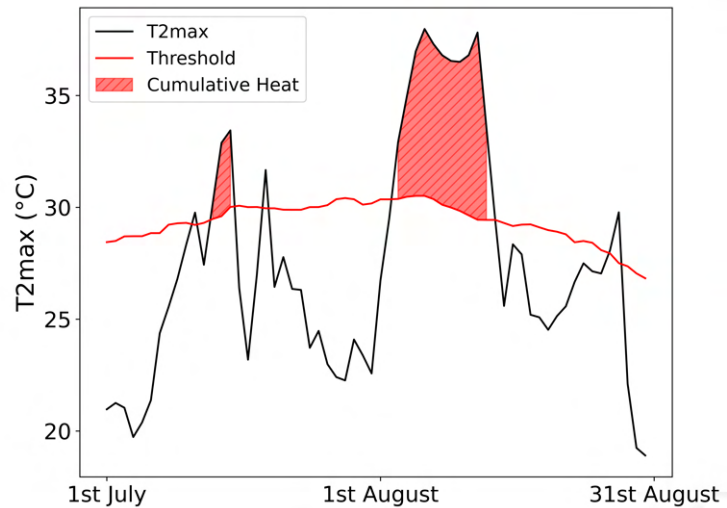


Figure 5: The cumulative heat for a specific grid-point in central France during 2003 July and August. The cumulative heat in the shaded red color is computed as the seasonal (July and August) integration of daily maximum temperatures (T_{2max} , black line) above the threshold (red line) during heatwave days. Heatwave days are identified when T_{2max} exceeds the 90th percentile based on a centered 15-day running window and 1982-2011 reference period for at least three consecutive days. ERA5 reanalysis data.

php/en/) and it led to several collaborations. In Rousi et al. (2022) we identify Europe as a heatwave hotspot and relate the recent increase in western EuSHWs to more persistent double jets over Eurasia. In Rousi et al. (2023) we elaborate a multi-faceted analysis of the 2018 EuSHW and show among other results that its occurrence was related to the spring North Atlantic tripolar pattern.

In the catalogue I show that my heatwave definition combined with the spatially integrated cumulative heat metric identifies the most severe recent EuSHW years. I list the ten EuSHW years with the highest cumulative heat and find that nine out of these ten belong to the second half of the study period starting in 2003, which highlights the recent increase of EuSHW intensity as shown in Rousi et al. (2022). The most recent year, 2022, is set as the second most intense EuSHW year after the year 2015. Other recent major heatwave cases such as the years 2003 and 2010, are within the ten strongest EuSHWs listed in the catalogue.

3 NORTH ATLANTIC SEA SURFACE TEMPERATURE ANOMALIES AS A PRECURSOR OF EUROPEAN SUMMER HEATWAVES: A CLIMATE MODEL-BASED APPROACH

With a suitable statistical method to identify the most intense EuSHW years, I proceed to relate their occurrence to the variability of spring North Atlantic sea surface temperatures (Beobide-Arsuaga et al. (2023), Appendix B). I apply the seasonally and interannually varying heatwave definition and the spatially integrated cumulative heat metric to MPI Grand-Ensemble historical simulations. From 15,600 historical years I select 5,000 years with the highest cumulative heat and 5,000 years

with the lowest cumulative heat. I refer to these two sets as EuSHW years and non-EuSHW years, respectively.

I develop a fully connected neural network model with the supervised task of differentiating the already identified EuSHW years and non-EuSHW years from April and May North Atlantic SSTAs (Fig. 3). The architecture of the neural network model is relatively simple with only three layers. The first layer is the input layer, where the standardized North Atlantic SSTAs are fit into the model in a vectorized form. The second layer is the only hidden layer with 20 neurons. The third layer is the output layer and consists of two neurons: one for EuSHW years and one for non-EuSHW years (more details in Beobide-Arsuaga et al. (2023), Appendix B). The output neurons provide the probability of a given spring North Atlantic SSTA field belonging to EuSHW years and non-EuSHW years. Although a more complex architecture with several hidden layers could potentially improve the performance of the neural network model, it would also hinder the interpretability of the results, and hence, the physical connection between spring North Atlantic SSTAs and the occurrence of EuSHWs.

Using spring North Atlantic SSTA fields as an input my neural network model is able to correctly classify 71% and 72% of EuSHW years and non-EuSHW years, respectively. A performance that is substantially higher than 50% indicates that the neural network model has found and learned patterns of the North Atlantic SSTAs that are related to the occurrence of EuSHWs. This brings us to the first question of my dissertation.

Which spring North Atlantic SSTA is a precursor of EuSHWs?

I find that the North Atlantic tripolar pattern with positive SSTAs in the Subtropical Gyre, and the positive regional SSTAs are a precursor of EuSHWs (Beobide-Arsuaga et al., 2023). The composite mean for correctly classified EuSHW years shows the North Atlantic tripolar pattern with positive SSTAs in the Subtropical Gyre and with negative SSTAs in the Subpolar Gyre and the tropical Atlantic. The composite mean also shows positive SSTAs in the regional seas around the European continent. In contrast, the composite mean of the correctly classified non-EuSHW years shows the opposite pattern. It shows the North Atlantic tripolar pattern with negative SSTAs in the Subtropical Gyre and with positive SSTAs in the Subpolar Gyre and the tropical Atlantic, and negative SSTAs in the regional seas around the European continent.

Furthermore, using layerwise relevance propagation I identify the positive regional SSTAs as the most important North Atlantic SSTAs to differentiate between EuSHW years and non-EuSHW years. The composite of the relevance maps highlights the positive SSTAs around the Iberian Peninsula, in the Mediterranean Sea, in the North Sea, and in the Baltic Sea preceding EuSHWs. A weaker relevance is also found for the positive SSTAs in the Subtropical Gyre. However, the composite contains distinct relevance patterns that highlight positive SSTAs in different regional seas as a precursor of distinct EuSHWs. Therefore, spring North Atlantic SSTAs besides indicating the occurrence of EuSHWs can also indicate their location. I apply the K-means clustering method (Hartigan and Wong, 1979) to classify the relevance maps into three groups and address my second research question.

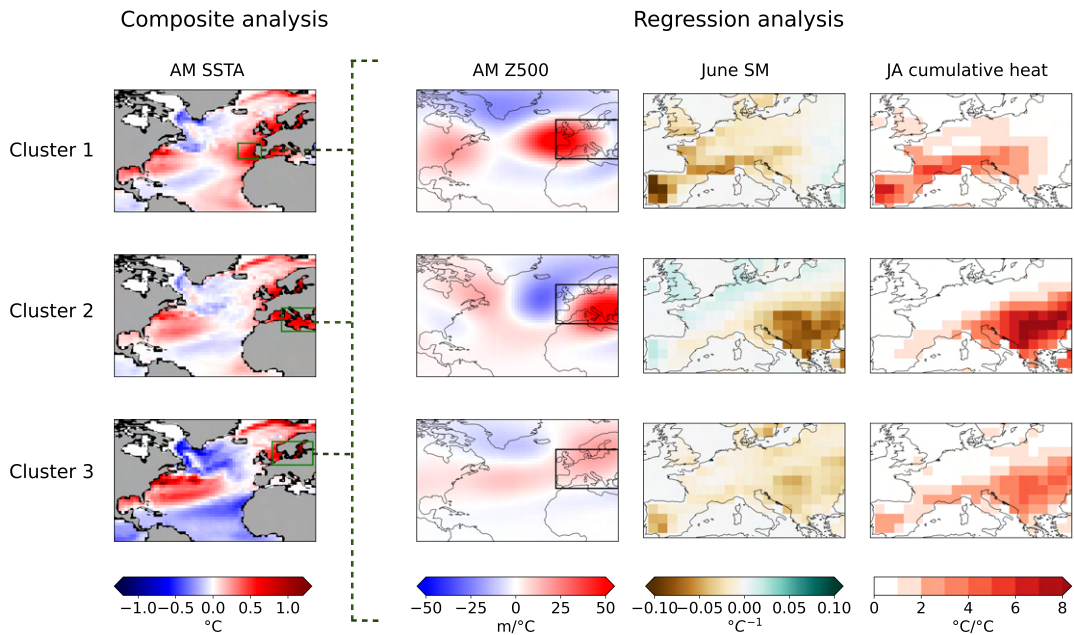


Figure 6: On the left, April and May (AM) mean sea surface temperature anomaly (SSTA) composites for the three clusters of layerwise relevance propagation clustering. Green boxes indicate the regions with the highest relevance for each cluster. On the right, linear regression analysis for AM mean SSTAs averaged over the green boxes on the left, and AM mean 500hPa geopotential height (Z500) anomalies, June soil moisture (SM) anomalies, and July and August (JA) heatwave intensity anomalies expressed as cumulative heat. Adapted from Beobide-Arsuaga et al. (2023).

Which spring North Atlantic SSTAs indicate the occurrence of EuSHWs, and which indicate the location?

I find that the phase of the spring North Atlantic tripolar pattern indicates the occurrence of EuSHWs and that positive spring SSTAs in different regional seas indicate the location of EuSHWs (Beobide-Arsuaga et al., 2023). The North Atlantic tripolar pattern with positive SSTAs in the Subtropical Gyre is a common feature that appears in all cluster composites, which indicates that it is a common precursor of EuSHWs (Fig. 6). However, the three clusters highlight distinct regional seas as the most relevant precursors of distinct EuSHWs. The composite mean of the first cluster indicates that positive SSTAs around the Iberian Peninsula are a precursor of western EuSHWs. The second cluster indicates that positive SSTAs in the Mediterranean Sea are a precursor of southeastern EuSHWs. The third cluster indicates that positive SSTAs in the North Sea and the Baltic Sea are also a precursor of southeastern EuSHWs albeit of less intensity.

Yet, the results described above are a product of statistical analysis and require a physical explanation that relates the spring North Atlantic tripolar pattern and regional SSTAs to the occurrence and location of EuSHWs.

Which physical mechanisms link the spring North Atlantic tripolar pattern and regional SSTAs to EuSHWs?

The spring North Atlantic tripolar pattern with positive SSTAs in the Subtropical Gyre relates in two ways to a deficit of winter and spring precipitation, leading to anomalously dry soil and preconditioning the occurrence of EuSHWs. On the one hand, we have an indirect relationship. The spring North Atlantic tripolar pattern is an expression of the previous winter North Atlantic Oscillation (Watanabe and Kimoto, 2000). A positive phase of the winter North Atlantic Oscillation is characterized by an increased sea level pressure gradient between the Azores high and the Icelandic low (Wanner et al., 2001). The increase in the gradient is accompanied by a northward shift of the storm-track and negative winter precipitation anomalies in southern Europe. On the other hand, we have a direct relationship. The North Atlantic tripolar pattern persists from winter to spring and creates a reversed ocean-to-atmosphere forcing (Chen et al., 2020; Czaja and Frankignoul, 1999, 2002; Gastineau and Frankignoul, 2015; Ossó et al., 2018). The change in meridional temperature gradient associated with the North Atlantic tripolar pattern affects the transient eddy activity, acting as a source of Rossby waves. Rossby waves affect the atmospheric flow leading to persistent high-pressure and negative spring precipitation anomalies over Europe (Song and Chen, 2023).

In addition, positive spring SSTAs in different regional seas enhance the persistence of high-pressure anomalies and the deficit of precipitation over different European regions, leading to distinct patterns of reduced soil moisture and conditioning the location of strongest EuSHWs (Fig. 6). With a linear regression analysis I show that positive spring SSTAs west of Iberian Peninsula are related to high-pressure anomalies, and negative spring precipitation and early-summer soil moisture anomalies in western Europe, amplifying the intensity of western EuSHWs. Positive spring SSTAs in the Mediterranean Sea are related to high-pressure anomalies, and negative spring precipitation and early-summer soil moisture anomalies in southeastern Europe, amplifying the intensity of southeastern EuSHWs. Positive spring SSTAs in the North Sea and Baltic Sea are related to high-pressure anomalies, and negative spring precipitation and early-summer soil moisture anomalies in southeastern Europe, amplifying the intensity of southeastern EuSHWs.

However, we should consider that the results described above are based on MPI Grand-Ensemble historical simulations, which run the low-resolution version of the MPI Earth System Model. A relatively coarse spatial resolution of the climate model might lead to spurious connections between the spring North Atlantic SSTAs and EuSHWs. Müller et al. (2018) showed that the increased model resolution reduces the biases of upper-level zonal winds and the position of the jet stream. The upper-level wind biases alter the propagation of Rossby waves induced by the North Atlantic SSTAs (Li et al., 2021), which modulate the atmospheric flow and precondition the occurrence of EuSHWs (Cassou et al., 2005; Kornhuber et al., 2020; Wulff et al., 2017). Moreover, the influence of the North Atlantic SSTAs in preconditioning the occurrence of EuSHWs might be affected by the ongoing increase of greenhouse gas emissions and the consequent changes in the climate. Therefore, I next investigate the applicability of the spring North Atlantic tripolar pattern and spring regional SSTAs to anticipate EuSHWs.

4 ON THE APPLICABILITY OF SPRING NORTH ATLANTIC SEA SURFACE TEMPERATURE ANOMALIES AS AN INDICATOR OF EUROPEAN SUMMER HEATWAVE OCCURRENCE

I employ the German Climate Forecast System (GFCS2.1; Fröhlich et al. (2021)), the fifth atmospheric reanalysis generation of ECMWF (ERA5; Hersbach et al. (2020)), and the European gridded land observational dataset (EOBS; Cornes et al. (2018)) and the Optimum Interpolation Sea Surface Temperature observational dataset (OISST; Huang et al. (2021)) for the period 1982-2022 to test the applicability of spring North Atlantic tripolar pattern and regional SSTAs as an indicator of EuSHW occurrence (Appendix C). GFCS2.1 is a seasonal forecast system based on the MPI high-resolution model (Müller et al., 2018), it has been operational since 2020 and consists of 30 ensemble members initialized in May. The ensemble members are initialized from the assimilation run, which is obtained by continuous nudging of atmospheric and oceanic conditions from the reanalysis data to bring the model close to the observed state of the climate system (Fröhlich et al., 2021).

After applying the seasonally-varying percentile-based heatwave definition and the cumulative heat metric, I use K-means clustering to separate the strongest EuSHW years with different spatial patterns from the weakest EuSHW years (see Appendix C). I obtain four clusters: the first cluster contains non-EuSHWs, the second cluster contains the strongest EuSHWs that affect the entire European domain, the third cluster contains western-EuSHWs, and the fourth cluster contains southeastern-EuSHWs.

I test if spring North Atlantic SSTAs favor the occurrence of EuSHWs focusing on the phase of the North Atlantic tripolar pattern and on the regional SSTAs: around the Iberian Peninsula, in the Mediterranean Sea, and in the North and Baltic Seas. I select 30% of the years with the most extreme spring SSTAs for each area of interest and compute the probability of EuSHW occurrence for each subset. If the probability ratio between the probability of EuSHW occurrence for each subset and the probability of EuSHW occurrence during the entire study period is above one, I determine that spring SSTAs are related to an increased likelihood of EuSHW occurrence.

Are the spring North Atlantic tripolar pattern and regional SSTAs related to the occurrence of EuSHWs in the GFCS2.1 seasonal forecast system?

I find that the spring North Atlantic tripolar pattern and regional SSTAs are related to the occurrence of EuSHWs in GFCS2.1 (Fig. 7a). The probability of EuSHW occurrence is increased with spring North Atlantic tripolar pattern with positive SSTAs in the Subtropical Gyre, or with positive spring SSTAs averaged over the regional seas. In contrast, the probability of EuSHW occurrence is decreased with spring North Atlantic tripolar pattern with negative SSTAs in the Subtropical Gyre, or with negative spring SSTAs averaged over the regional seas. Furthermore, the occurrence of EuSHWs is more related to regional SSTAs than to the phase of the North Atlantic tripolar pattern. The increase of EuSHW occurrence probability is higher with positive SSTAs averaged over the regional seas than with the North Atlantic tripolar pattern with positive SSTAs in the Subtropical Gyre.

The probability of western and southeastern EuSHW occurrence is also increased with the spring North Atlantic tripolar pattern with positive SSTAs in the Subtropi-

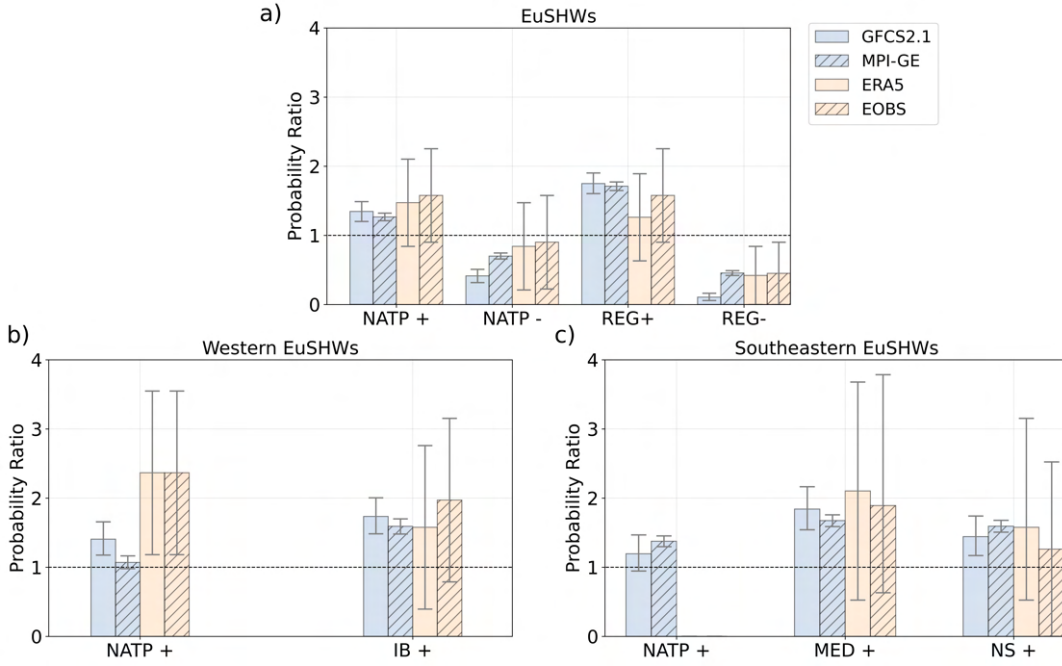


Figure 7: For GFCS2.1, MPI Grand-Ensemble historical simulations (MPI-GE), ERA5 reanalysis dataset, and EOBS and OISST observational datasets (OBS); **(a)** The probability of European summer heatwave (EuSHW) occurrence relative to the climatology for the upper (+) and lower (-) 30th percentile of April and May mean North Atlantic tripolar pattern (NATP) index and regional SSTAs (REG); **(b)** The probability of western EuSHW occurrence relative to the climatology for the upper 30th percentile of the NATP index and the SSTAs surrounding the Iberian Peninsula (IB); **(c)** The probability of southeastern EuSHW occurrence relative to the climatology for the upper 30th percentile of the NATP index, the SSTAs in the Mediterranean Sea (MED), and the SSTAs in the North and Baltic Seas (NS). The NATP index is computed as the SSTA difference between the Subtropical Gyre (80°W-60°W, 25°N-35°N) and the Subpolar Gyre (40°W-25°W, 45°N-55°N). REG is computed as the SSTAs averaged over the three regional domains: IB (12°W-5°E, 33°N-47°N), MED (5°E-28°E, 30°N-45°N) and NS (3°W-28°E, 50°N-65°N). The uncertainties are computed with a 90% confidence after bootstrapping over each SSTA subset.

cal Gyre, which indicates that it is a common indicator of the occurrence of different EuSHWs (Fig. 7b,c). However, the occurrence of western EuSHW is more likely with positive spring SSTAs around the Iberian Peninsula (Fig. 7b), and the occurrence of southeastern EuSHWs is more likely with positive SSTAs in the Mediterranean Sea and in the North and Baltic Seas, in the respective order (Fig. 7c).

The results obtained from GFCS2.1 are in general agreement with the ones obtained from the MPI Grand-Ensemble historical simulations (Fig. 7). The agreement indicates that regardless of the different study periods, resolution of the models, or the initialization of the seasonal forecast system, in both datasets the spring North Atlantic tripolar pattern with positive SSTAs in the Subtropical Gyre and positive regional SSTAs are related to the occurrence of EuSHWs.

Are the spring North Atlantic tripolar pattern and regional SSTAs related to the occurrence of EuSHWs in reanalysis and observational datasets?

I find that the North Atlantic tripolar pattern with positive SSTAs in the Subtropical Gyre, and the positive SSTAs in the regional seas are related to the increased probability of EuSHW occurrence in ERA5 and observational datasets (Fig. 7a). In contrast, the negative SSTAs in the regional seas are related to the decreased probability of EuSHWs occurrence. The probability of EuSHW occurrence does not considerably change with the North Atlantic tripolar pattern with negative SSTAs in the Subtropical Gyre.

Furthermore, not all EuSHWs are related to the North Atlantic tripolar pattern with positive SSTAs in the Subtropical Gyre as shown by GFCS2.1. While the probability of western-EuSHW occurrence is increased (Fig. 7b), the probability of southeastern-EuSHWs occurrence is practically zero (Fig. 7c). Similarly as in GFCS2.1, western and southeastern EuSHWs are related to positive SSTAs in different regional seas. The occurrence of western-EuSHWs is increased with positive SSTAs around the Iberian Peninsula, albeit in less magnitude than with the North Atlantic tripolar pattern with positive SSTAs in the Subtropical Gyre. The occurrence of southeastern-EuSHWs is mostly increased with positive SSTAs in the Mediterranean Sea, and in less magnitude with positive SSTAs in the North and Baltic Seas.

The main disagreement between GFCS2.1, and ERA5 and observational datasets arise from the North Atlantic tripolar pattern. While in GFCS2.1 the North Atlantic tripolar pattern with positive SSTAs in the Subtropical Gyre indicates the occurrence of western and southeastern-EuSHWs, in ERA5 and observational datasets the North Atlantic tripolar pattern with positive SSTAs in the Subtropical Gyre indicates the occurrence of only western-EuSHWs. In addition, while in GFCS2.1 the North Atlantic tripolar pattern with positive SSTAs in the Subtropical Gyre is less related to western-EuSHWs than the positive SSTAs around the Iberian Peninsula, the inverse is true for ERA5 and observational datasets. The disagreements indicate that GFCS2.1 misses predicting western-EuSHWs and falsely predicts southeastern-EuSHWs with the North Atlantic tripolar pattern with positive SSTAs in the Subtropical Gyre.

The agreement between GFCS2.1, and ERA5 and observational datasets allows me to robustly state that spring North Atlantic SSTAs are applicable to anticipate EuSHWs. In all datasets, I find that the probability of western EuSHW occurrence is increased with the spring North Atlantic tripolar pattern with positive SSTAs in the Subtropical Gyre and with positive SSTAs around the Iberian Peninsula. Furthermore, all datasets agree that the probability of southeastern EuSHW occurrence is increased with positive spring SSTAs in the Mediterranean Sea, and in the North and Baltic Seas. In contrast, the probability of EuSHW occurrence is reduced with negative SSTAs averaged over the regional seas.

5 CONCLUSIONS AND OUTLOOK

This dissertation aims towards anticipating the occurrence of EuSHWs a season in advance by relating their occurrence to spring North Atlantic SSTAs. Several case studies have suggested that different North Atlantic SSTAs influenced the occurrence of past EuSHWs (Duchez et al., 2016; Feudale and Shukla, 2007, 2011; Wulff et al., 2017), but the limited number of observed events associated with several

physical mechanisms has prevented a robust identification of spring North Atlantic SSTAs as precursors. Here, I combine 100 historical simulations of the MPI Grand-Ensemble (1850-2005), neural networks, and layerwise relevance propagation, to robustly identify for the first time the most important North Atlantic SSTAs as precursors of different EuSHWs (Beobide-Arsuaga et al. (2023), Appendix B).

I find that the North Atlantic tripolar pattern with positive SSTAs in the Subtropical Gyre, and negative SSTAs in the Subpolar Gyre and the tropical Atlantic is a common precursor of EuSHWs. The North Atlantic tripolar pattern is related to negative winter and spring precipitation anomalies over Europe, which reduce the soil moisture and precondition the occurrence of EuSHWs (Fischer et al., 2007; Gastineau and Frankignoul, 2015; Song and Chen, 2023; Wanner et al., 2001; Watanabe and Kimoto, 2000). In addition, I find that positive SSTAs in different regional seas around Europe are precursors of distinct EuSHWs. While positive SSTAs around the Iberian Peninsula are a precursor of western-EuSHWs, positive SSTAs in the Mediterranean Sea and in the North and Baltic Seas are a precursor of southeastern-EuSHWs. Positive regional SSTAs relate to distinct persistent high-pressure and negative precipitation anomalies, leading to distinct patterns of reduced soil moisture in early summer and amplifying the intensity of EuSHWs in different European regions.

However, the MPI Grand-Ensemble historical simulations which run the low-resolution version of the MPI climate model, might lead to unrealistic relationships between spring North Atlantic SSTAs and the occurrence of EuSHWs due to model biases (Müller et al., 2018). I test the applicability of spring North Atlantic tripolar pattern and regional SSTAs to anticipate recent EuSHWs in GFCS2.1 seasonal forecast system, in ERA5 reanalysis product, and in EOBS and OISST observational datasets for the period 1982-2022 (Appendix C).

I find that GFCS2.1, albeit running the high-resolution version of the MPI climate model, being initialized in May, and covering a different time period, is in general agreement with MPI Grand-Ensemble historical simulations. The probability of EuSHW occurrence is increased with the spring North Atlantic tripolar pattern with positive SSTAs in the Subtropical Gyre. In addition, the probability of western and southeastern EuSHWs is increased with positive spring SSTAs around the Iberian Peninsula, and with positive SSTAs in the Mediterranean, North and Baltic Seas, respectively. In all cases, the probability of EuSHW occurrence is higher with positive spring regional SSTAs than with the North Atlantic tripolar pattern with positive SSTAs in the Subtropical Gyre.

In contrast, ERA5 and observational datasets indicate that the spring North Atlantic tripolar pattern with positive SSTAs in the Subtropical Gyre does not indicate the occurrence of all EuSHWs. While the occurrence of western-EuSHWs is increased with the North Atlantic tripolar pattern with positive SSTAs in the Subtropical Gyre, the occurrence of southeastern-EuSHWs is practically zero. Furthermore, I find that the probability of western-EuSHW occurrence is higher with the North Atlantic tripolar pattern with positive SSTAs in the Subtropical Gyre than with positive SSTAs around the Iberian Peninsula.

The discrepancies between GFCS2.1, and ERA5 and observational datasets suggest that some ensemble members of GFCS2.1 misrepresent the influence of the North Atlantic tripolar pattern on European summer climate, in agreement with

Neddermann et al. (2019). The identified discrepancies offer a new possibility to improve the seasonal predictability of EuSHWs by sub-selecting the ensemble members that capture the realistic connection between the North Atlantic tripolar pattern and EuSHWs (Dobrynin et al., 2018; Neddermann et al., 2019).

Independent of improving the seasonal prediction system, the agreement between GFCS2.1, ERA5, and observational datasets allows me to robustly indicate which spring North Atlantic SSTAs are applicable to anticipate the occurrence of EuSHWs. In all datasets, I find that the probability of western-EuSHWs is increased with the spring North Atlantic tripolar pattern with positive SSTAs in the Subtropical Gyre, and with positive SSTAs around the Iberian Peninsula. Furthermore, the probability of southeastern-EuSHWs is increased with positive spring SSTAs in the Mediterranean, North, and Baltic Seas. In contrast, the occurrence of EuSHWs is unlikely with negative spring SSTAs averaged over the regional seas.

The methodology applied in this dissertation can be used to investigate other possible relevant precursors of EuSHWs in order to better estimate their occurrence. As an example, Kneller (2023) combined the historical MPI Grand-Ensemble simulations, neural networks, and layerwise relevance propagation to show that a spring Arctic sea-ice dipolar pattern with negative anomalies north of Eurasia and positive anomalies north of North America is also a precursor of EuSHWs. Yet, the applicability of the spring Arctic sea-ice dipolar pattern to anticipate the occurrence of EuSHWs should be tested in reanalysis and observational datasets. In addition, the relationship between spring Arctic sea-ice anomalies and the North Atlantic SSTAs to influence the occurrence of EuSHWs remains to be investigated.

The outcome of the present dissertation can result in a relevant societal benefit. The spring North Atlantic tripolar pattern and regional SSTAs, and potentially the spring Arctic sea-ice dipolar pattern, could be used to develop a seasonal early warning system of EuSHWs. The seasonal early warning system could be set to inform the vulnerable sectors about the probability of EuSHW occurrence based on the identified North Atlantic SSTAs. As a consequence, it would increase preparedness and potentially reduce the damages and economic losses related to EuSHWs (Merz et al., 2020).

APPENDICES



EUROPEAN SUMMER HEATWAVE CATALOGUE

The report in this appendix contains a European summer heatwave catalogue, which has been part of my contribution to the ClimXtreme project (<https://climxtreme.net/index.php/en/>). The data used to create the catalogue has been published as:

Beobide-Arsuaga, G. (2023). "European summer heatwave catalogue". DOKU at DKRZ. https://www.wdc-climate.de/ui/entry?acronym=DKRZ_LTA_1075_ds00028.

European summer heatwave catalogue

Goratz Beobide-Arsuaga^{1,2}

¹Institute of Oceanography, Center for Earth System Research and Sustainability (CEN), Universität Hamburg, Hamburg, Germany

²International Max Planck Research School on Earth System Modelling, Max Planck Institute for Meteorology, Hamburg, Germany

1 INTRODUCTION

The present report contains a European summer heatwave catalogue between 1982 and 2022. The catalogue is elaborated from ERA5 global atmospheric reanalysis product. A seasonally-varying percentile-based definition is used to identify European summer heatwaves and the cumulative heat metric is used to assess the intensity. The catalogue provides the cumulative heat of European summer heatwaves for each study year and a list of the ten most intense heatwave years. In addition, the cumulative heat and the list of the ten most intense heatwave years are provided for different European sub-domains: north-west, central-west, Iberian Peninsula, south-east, north-east, and Germany.

2 DATA AND METHODS

2.1 Data

The catalogue employs ERA5 global atmospheric reanalysis product for the years between 1982 and 2022. The original dataset is linearly interpolated to T₁₂₇ spectral resolution. Heatwaves are identified during high boreal summer (July and August) using daily maximum surface temperatures (T_{2max}). Europe is here defined as 10°W-30°E, 35°N-60°N. In addition, following the European heatwave classification by Stefanon et al. (2012) Europe is divided into six sub-domains: north-west (10°W-6°E, 50°N-60°N), central-west (5°W-6°E, 44°N-50°N), Iberian Peninsula (10°W-6°E, 36°N-44°N), south-east (6°E-30°E, 36°N-47°N), north-east (6°E-30°E, 47°N-60°N), and Germany (6°E-15°E, 47°N-55°N).

2.2 Methods

Heatwaves are here identified on a grid-point level when T_{2max} exceeds the 90th percentile based on a centered 15-day running window and 1982-2011 reference period for at least three consecutive days (Perkins and Alexander, 2013). The intensity of heatwaves is expressed with the cumulative heat metric (Perkins-Kirkpatrick and Lewis, 2020). The cumulative heat is the seasonal integration of T_{2max} above the threshold during heatwave days. Here the cumulative heat is additionally integrated over the spatial domain after weighting each grid-point by the cosine of

its latitude. The output is a single number per year that expresses the intensity of heatwaves for each area of interest. The ten most intense heatwave years are listed in decreasing order.

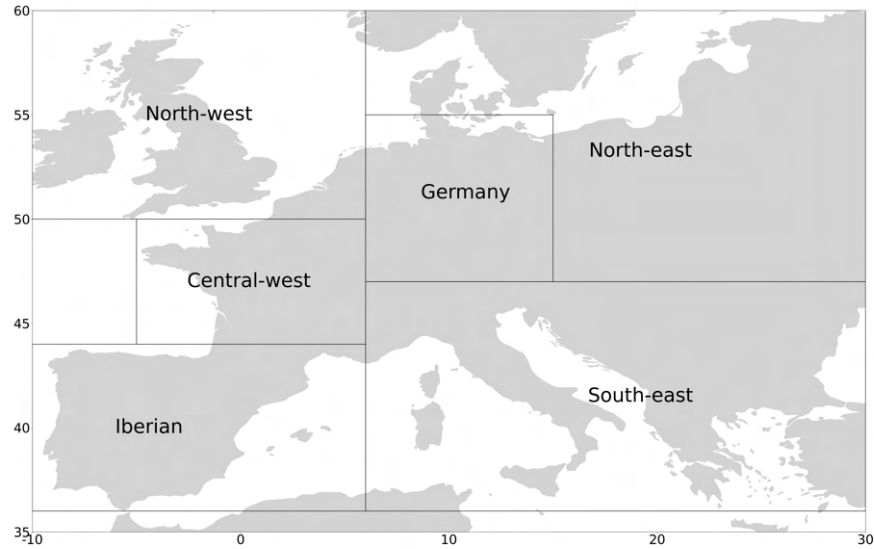


Figure A.1: Representation of the study area (10°W - 30°E , 35°N - 60°N) and the selected sub-domains: north-west (10°W - 6°E , 50°N - 60°N), central-west (5°W - 6°E , 44°N - 50°N), Iberian Peninsula (0°W - 6°E , 36°N - 44°N), south-east (6°E - 30°E , 36°N - 47°N), north-east (6°E - 30°E , 47°N - 60°N), and Germany (6°E - 15°E , 47°N - 55°N).

3 EUROPEAN SUMMER HEATWAVE CATALOGUE

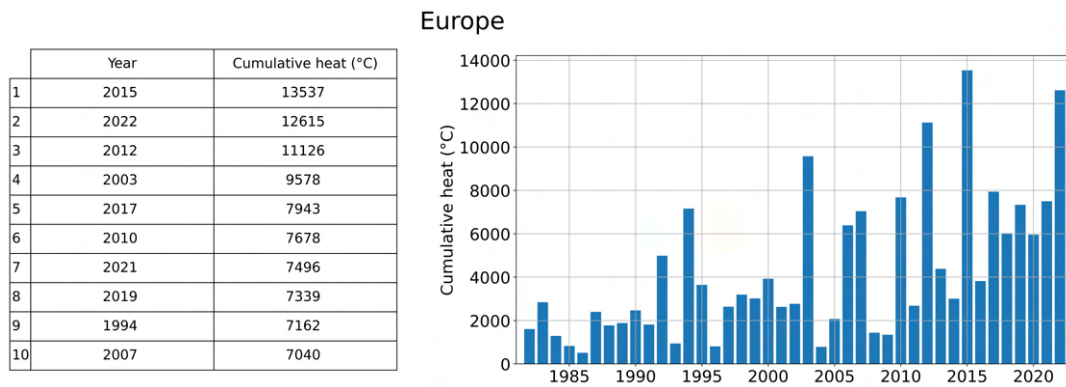


Figure A.2: European (10°W - 30°E , 35°N - 60°N) summer heatwave catalogue with the cumulative heat for each study year (1982-2022) and with a list of the ten most intense heatwave years.

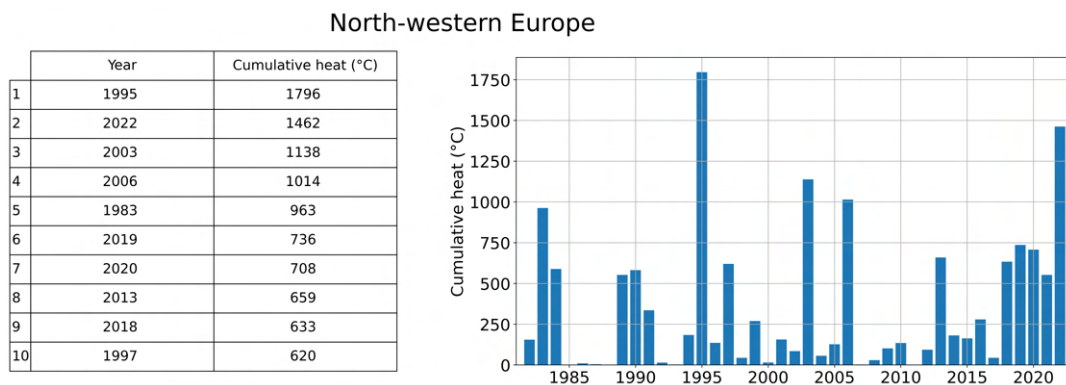


Figure A.3: North-western European (10°W - 6°E , 50°N - 60°N) summer heatwave catalogue with the cumulative heat for each study year (1982-2022) and with a list of the ten most intense heatwave years.

Central-western Europe

	Year	Cumulative heat (°C)
1	2003	2606
2	2022	1712
3	2019	1275
4	2015	1186
5	2020	1063
6	2016	851
7	1990	816
8	2006	792
9	2018	692
10	2017	651

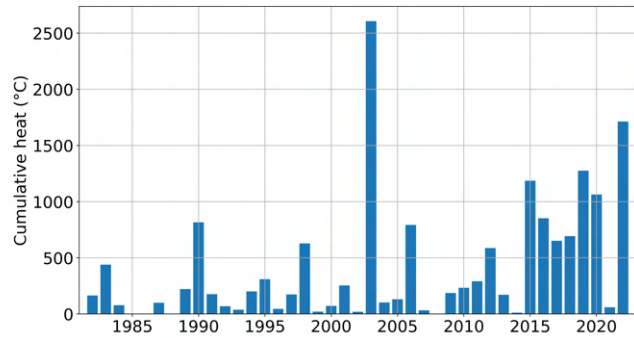


Figure A.4: Central-western European (5°W-6°E, 44°N-50°N) summer heatwave catalogue with the cumulative heat for each study year (1982-2022) and with a list of the ten most intense heatwave years.

Iberian

	Year	Cumulative heat (°C)
1	2022	2629
2	2003	1535
3	2015	1181
4	2012	1097
5	2020	1044
6	2021	1031
7	2017	954
8	2018	767
9	1991	729
10	2019	656

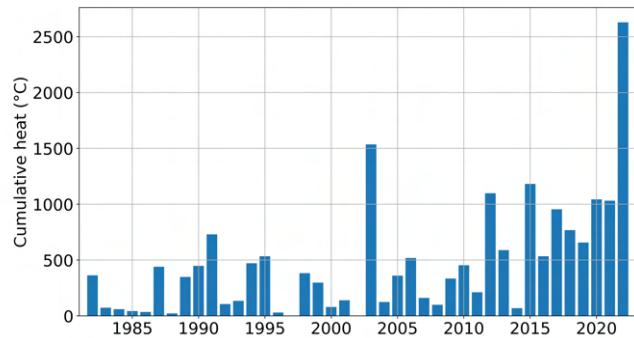


Figure A.5: Iberian (10°W-6°E, 36°N-44°N) summer heatwave catalogue with the cumulative heat for each study year (1982-2022) and with a list of the ten most intense heatwave years.

South-eastern Europe

	Year	Cumulative heat (°C)
1	2012	4635
2	2007	4015
3	2017	3634
4	2021	3227
5	2015	2830
6	2000	2571
7	2022	1831
8	2003	1681
9	1987	1541
10	1998	1518

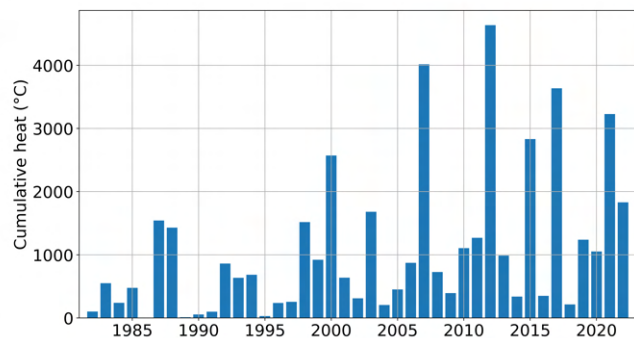


Figure A.6: South-eastern European (6°E-30°E, 36°N-47°N) summer heatwave catalogue with the cumulative heat for each study year (1982-2022) and with a list of the ten most intense heatwave years.

North-eastern Europe

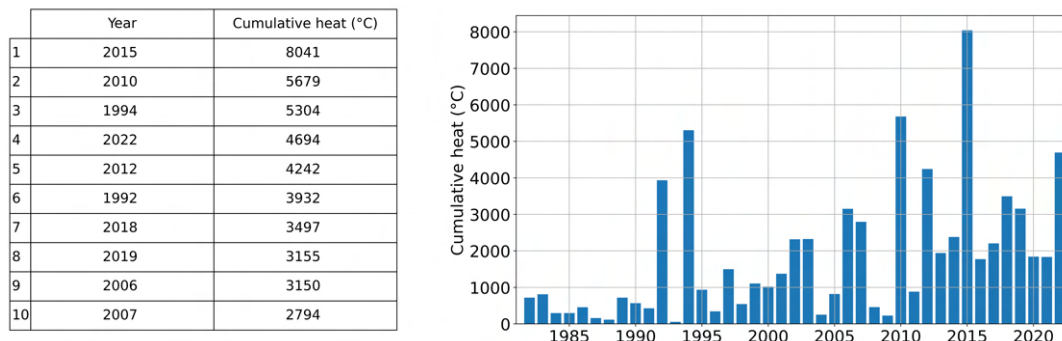


Figure A.7: North-eastern European (6°E-30°E, 47°N-60°N) summer heatwave catalogue with the cumulative heat for each study year (1982-2022) and with a list of the ten most intense heatwave years.

Germany

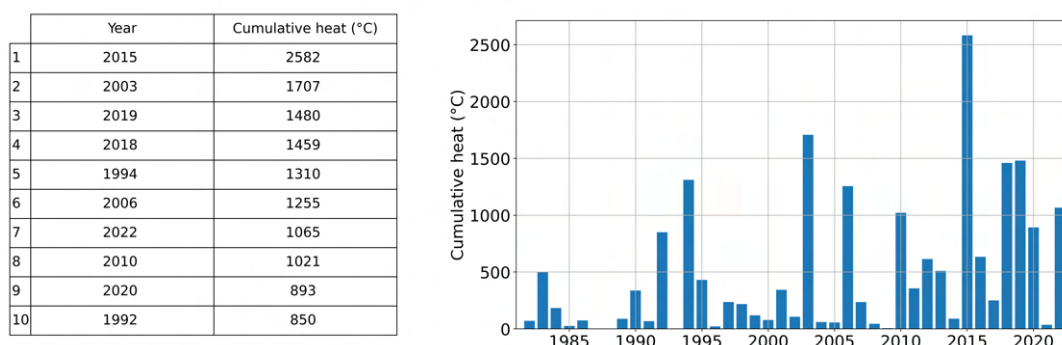


Figure A.8: German (6°E-15°E, 47°N-55°N) summer heatwave catalogue with the cumulative heat for each study year (1982-2022) and with a list of the ten most intense heatwave years.

SPRING REGIONAL SEA SURFACE TEMPERATURES AS A PRECURSOR OF EUROPEAN SUMMER HEATWAVES

The work in this appendix has been published as:

Beobide-Arsuaga, G., Düsterhus, A., Müller, W. A., Barnes, E. A., and Baehr, J. (2023). "Spring Regional Sea Surface Temperatures as a Precursor of European Summer Heatwaves". *Geophysical Research Letters*, 50(2), e2022GL100727, <https://doi.org/10.1029/2022GL100727>.

The contribution to this paper is as follows: G.B.-A., A.D., W.A.M., E.A.B, and J.B. conceived and designed the study. G.B.-A. performed the analysis and wrote the paper. A.D., W.A.M., E.A.B., and J.B. contributed through discussions and reviewed the manuscript.

Spring Regional Sea Surface Temperatures as a Precursor of European Summer Heatwaves

Goratz Beobide-Arsuaga^{1,2}, André Düsterhus³, Wolfgang A. Müller⁴,
Elizabeth A. Barnes⁵ and Johanna Baehr¹,

¹Institute of Oceanography, Center for Earth System Research and Sustainability (CEN), Universität Hamburg, Hamburg, Germany

²International Max Planck Research School on Earth System Modelling, Max Planck Institute for Meteorology, Hamburg, Germany

³Maynooth University, ICARUS, Department of Geography, Maynooth, Ireland

⁴Max Planck Institute for Meteorology, Ocean in the Earth System, Hamburg, Germany

⁵Department of Atmospheric Science, Colorado State University, Fort Collins, CO, USA

Received: 19 August 2022 / Accepted: 07 January 2023 / Published online: 17 January 2023

ABSTRACT

Different spring and early summer North Atlantic sea surface temperature anomalies (SSTAs) have been shown to precede recent European summer heatwaves (EuSHWs). So far, the limited number of observed events associated with several physical mechanisms has prevented a robust identification of SSTAs as precursors. Here, we extend beyond previous studies by combining 100 historical simulations (1850–2005) of the MPI Grand-Ensemble with an explainable neural-network method. We find that the spring tripolar North Atlantic pattern with positive SSTAs in the Subtropical Gyre is a precursor of EuSHWs. In addition, positive SSTAs west of the Iberian Peninsula, and in the North Sea, the Baltic Sea and the Mediterranean Sea relate to distinct early summer soil moisture anomaly patterns and are precursors of western and southeastern EuSHWs, respectively. While the phase of the tripolar North Atlantic pattern indicates whether a EuSHW might emerge, regional SSTAs indicate the spatial characteristics of EuSHWs.

PLAIN LANGUAGE SUMMARY

Past studies have investigated the influence of spring and early summer North Atlantic sea surface temperature anomalies (SSTAs) on recent European summer heatwaves (EuSHWs). These studies have proposed different SSTAs in the North Atlantic as the most important for the development of different EuSHWs. Yet, it has not been possible to generalize which spring North Atlantic SSTAs are the

most important to anticipate EuSHWs because we have too few observed events and they showed different spatial and physical characteristics. Here, we analyze 100 historical simulations (1850–2005) of the MPI Grand-Ensemble in which we identify a large number of EuSHWs. We use an explainable neural-network method to find which spring North Atlantic SSTAs are the most important to anticipate EuSHWs. We find that warm SSTAs in the Subtropical Gyre surrounded by cold SSTAs in the north and in the south is an indicator of EuSHW occurrence. In addition, different regional SSTAs relate to drier than normal soil moisture in different parts of Europe that influence different EuSHWs. Warm SSTAs west of the Iberian Peninsula, and in the North Sea, the Baltic Sea and the Mediterranean Sea indicate the occurrence of western and southeastern EuSHWs, respectively.

1 INTRODUCTION

The large-scale oceanic and atmospheric dynamics in the North Atlantic are thermally coupled on an interannual timescale (Bjerknes, 1964; Watanabe and Kimoto, 2000). Furthermore, the coupling also occurs on a seasonal timescale. While the winter North Atlantic Oscillation (NAO) acts as a main driver imprinting spring tripolar North Atlantic sea surface temperature anomalies (SSTA), persistent SSTAs in-turn affect the atmospheric flow and can potentially precondition European summer heatwaves (EuSHWs) (Czaja and Frankignoul, 2002; Ossó et al., 2018). The tripolar SSTA pattern has been related to anticyclonic anomalies over Europe (Gastineau and Frankignoul, 2015), increasing the temperatures and decreasing precipitation by compressing the downward moving air, and blocking the westerlies and the intrusion of storm track (Rex, 1950; Treidl et al., 1981). In the case of long-lasting blocking, the soil moisture (SM) in the region decreases, reducing the latent cooling in the atmosphere and further increasing air temperatures (Fischer et al., 2007; Seneviratne et al., 2006).

The SSTAs in the Subpolar Gyre (SPG) and tropical Atlantic, both part of the tripolar North Atlantic pattern, have been related to the 2015 EuSHW (Duchez et al., 2016; Wulff et al., 2017). Duchez et al. (2016) suggested that the negative SSTAs in the SPG were responsible for the southward shift of the Jet Stream, which enhanced the blocking anticyclone over Central Europe and lead to the 2015 EuSHW. In contrast, Wulff et al. (2017) proposed that the negative SSTAs in the tropical Atlantic, and the respective diabatic heating anomalies, were responsible for the blocking system and hence, the 2015 EuSHW.

In addition to North Atlantic SSTAs, surface temperatures in different European regional seas have also been proposed to precede EuSHWs. According to Feudale and Shukla (2011), positive SSTAs in the North Sea reduced the meridional temperature gradient and baroclinic activity, allowing the blocking to persist over Europe during the 2003 EuSHW. The dominant descending motion prevented convection and increased temperatures warming the Mediterranean Sea. Positive SSTAs in the Mediterranean Sea have been related to dry and warm European summers, and are thought to be responsible for half of the amplitude of the 2003 EuSHW (Feudale and Shukla, 2007; Ionita et al., 2017).

The limited number of observed EuSHW events associated with a variety of physical mechanisms has prevented the systematic identification of SSTAs as precursors

of EuSHWs. The MPI Grand-Ensemble (MPI-GE) data set combined with a neural-network (NN) based explainable artificial intelligence method, layerwise relevance propagation (LRP) (Bach et al., 2015; Toms et al., 2020), provides a unique opportunity for a systematic analysis of EuSHW precursors. Here, we robustly identify the most important spring North Atlantic SSTAs as precursors of different EuSHWs.

2 DATA AND METHODS

2.1 Data

We use the 100-member MPI-GE with historical anthropogenic and natural forcing (1850–2005), and high temporal resolution (Maher et al., 2019). The 100 ensemble members use the same model set-up and forcing, but are started from different initial conditions all taken from the quasi-equilibrated control-run (Maher et al., 2019). MPI-GE includes the land component JSBACH with a five-layer scheme improving the representation of soil hydrological processes (Hagemann and Stacke, 2015). The MPI-GE uses the low resolution version of the MPI-ESM model, which represents well the observed connection between spring North Atlantic SSTA and Eurasian surface temperatures via atmospheric wave trains, as well as the observed frequency and amplitude of extreme European summer temperatures (Chen et al., 2021; Suarez-Gutierrez et al., 2018).

We analyze the following climate variables: daily surface maximum temperature (T_{2max}) and monthly sea surface temperature (SST), total precipitation (TP), geopotential height at 500 hPa (Z_{500}) and SM. SM is here defined as the fraction of water accumulated in the root zone relative to the water capacity for each grid-point. We compute monthly anomalies relative to a centered 31-year moving climatology. The results are insensitive to the residual linear trend.

2.2 Identification and Quantification of Heatwaves

We identify heatwaves during high summer (July and August, hereafter JA). For each land grid-point and calendar day, we use a percentile based heatwave definition (Perkins and Alexander, 2013). Heatwaves are defined when T_{2max} exceeds the 90th percentile based on a centered 15-day, 31-year running window for at least three consecutive days. Hence, our heatwave definition considers spatial differences and temporal (both seasonal and long-term) variability of the threshold. A temporally fixed threshold would overestimate the identification of heatwaves during the climatological peak (i.e., August) and at the end of the historical run due to increasing temperatures driven by global warming.

The intensity of heatwaves is expressed as cumulative heat (Perkins-Kirkpatrick and Lewis, 2020). The cumulative heat is obtained by seasonal (JA) integration of heat exceeding the defined threshold during heatwave days. We additionally integrate the cumulative heat over the European domain ($10^{\circ}W$ – $30^{\circ}E$, 35 – $60^{\circ}N$) after weighting each grid-point by the cosine of its latitude, obtaining a single value per year representing the intensity of EuSHWs. We evaluate the cumulative heat of 15,600 historical summers and select 10,000 years: 5,000 years with highest cumula-

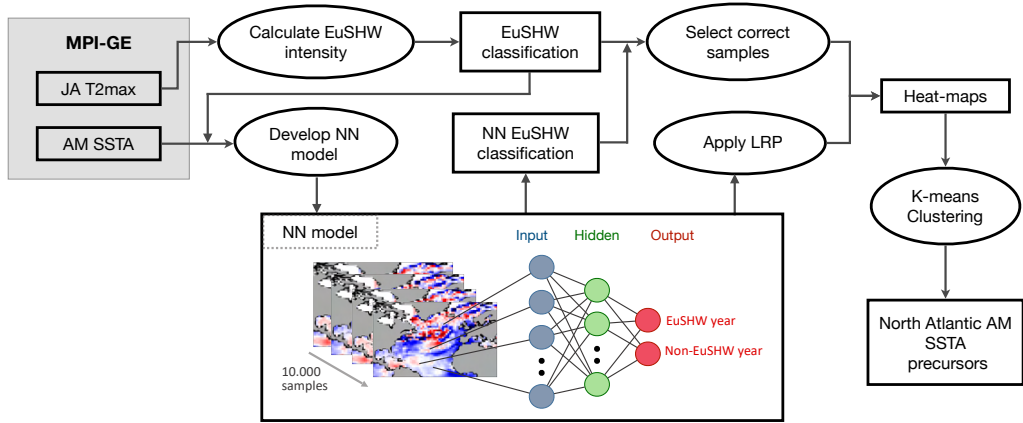


Figure B.1: Schematic representation of the methodology employed here to identify North Atlantic spring (April and May; AM) sea surface temperature anomalies as a precursor of European summer (July and August; JA) heatwaves (EuSHWs) using neural-network (NN) based explainable artificial intelligence method, layerwise relevance propagation (LRP).

tive heat and 5,000 years with lowest cumulative heat. We consider these two sets as EuSHW years and non-EuSHW years, respectively.

2.3 Neural-Network Set-Up

We develop a fully connected NN model (Lecun et al., 2015) for a supervised classification of the previously selected 10,000 years (Section 2.2) using spring (April and May, hereafter AM) mean North Atlantic (100°W – 30°E , 0 – 80°N) SSTAs (Figure B.1). Our NN contains three layers. The first layer is the input layer, where we insert standardized AM North Atlantic SSTAs in a vectorized form (1,584 features). The second layer is the hidden layer and contains 20 neurons with rectified linear unit (Relu) activation function. We use L2 regularization with coefficient 2.0 to avoid overfitting. The third layer is the output layer and it has two neurons: one for EuSHW years and one for non-EuSHW years. We apply the softmax operator to obtain the probability of each sample belonging to the EuSHW and non-EuSHW years. The output neuron with highest probability determines the NN EuSHW classification. We train the model with 80% randomly shuffled samples and validate with the remaining 20%. A slightly different selection of hyperparameters and different methods of splitting the training and validation sets (i.e., splitting the time dimension in chunks of five consecutive years or splitting the ensemble dimension) do not influence the findings of this paper.

We evaluate the model performance by comparing the NN EuSHW classification to the EuSHW classification introduced in Section 2.2, and select the correctly classified samples. We use LRP to obtain one heat-map per correctly classified sample highlighting which grid-points from the input layer are most relevant to differ-

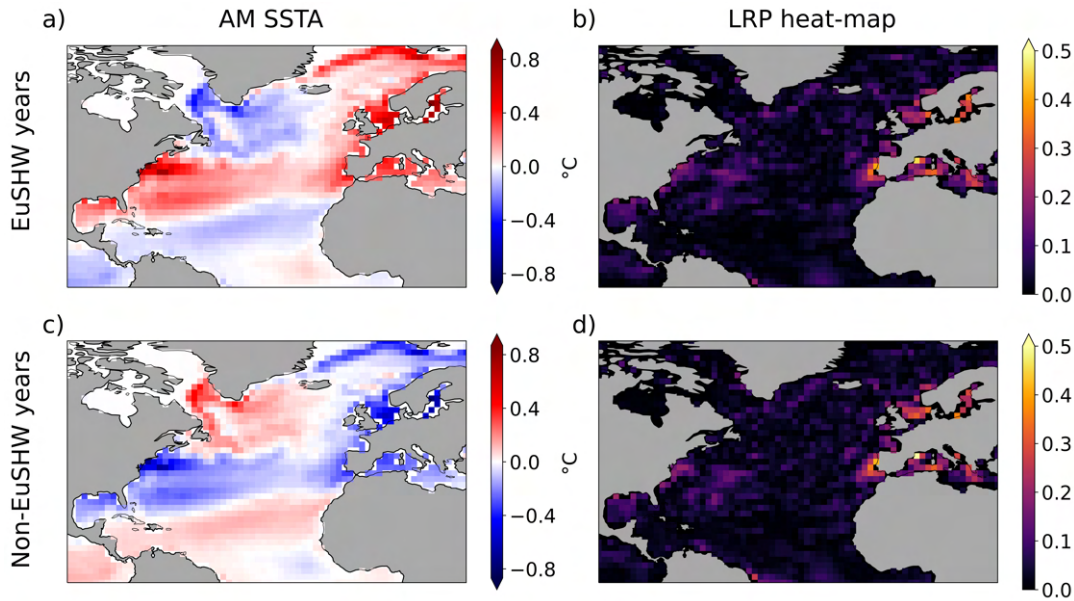


Figure B.2: April and May (AM) mean SSTA composites of correctly classified; **(a)** European summer heatwave (EuSHW) years; **(c)** non-EuSHW years. Layerwise relevance propagation (LRP) heat-map composites of correctly classified; **(b)** EuSHW years; **(d)** non-EuSHW years. LRP composites are computed after normalizing each sample between 0 and 1.

entiate between EuSHW and non-EuSHW years. We use K-means (Hartigan and Wong, 1979) to cluster the LRP relevance patterns of correctly classified EuSHW years with model confidence above 60%, and to identify the most important North Atlantic SSTAs as a precursor of different EuSHWs (Mayer and Barnes, 2021). The results are insensitive to the selection of the confidence threshold.

3 RESULTS

Our NN model correctly classifies 71% and 72% of EuSHW and non-EuSHW years: 3,567 and 3,598 samples, respectively. The performance is similar both in training and validation sets indicating that the model does not overfit. AM SSTA composites of correctly classified samples show that the tripolar North Atlantic pattern with opposite phases leads to EuSHW and non-EuSHW years (Figures B.2a and B.2c). Negative SSTAs in the SPG and the tropical Atlantic, and positive SSTAs in the Subtropical Gyre precede summers classified as EuSHW years (Figure B.2a). In contrast, positive SSTAs in the SPG and tropical Atlantic, and negative SSTAs in the Subtropical Gyre precede summers classified as non-EuSHW years (Figure B.2c).

Twenty-nine percent of EuSHW years that our model incorrectly classifies as non-EuSHW years, mainly the least intense EuSHW years (Figure B.5 in Supplementary Information 5), indicate that other processes besides North Atlantic SSTAs play a role in the development of EuSHWs. Weiland et al. (2021) demonstrated that the European summer atmospheric circulation depends on its early summer atmospheric state, which can persist for up to 45 days and could lead to a heatwave. In addition, Mecking et al. (2019) showed that matching atmospheric and sea-ice conditions were fundamental for the 2015 EuSHW.

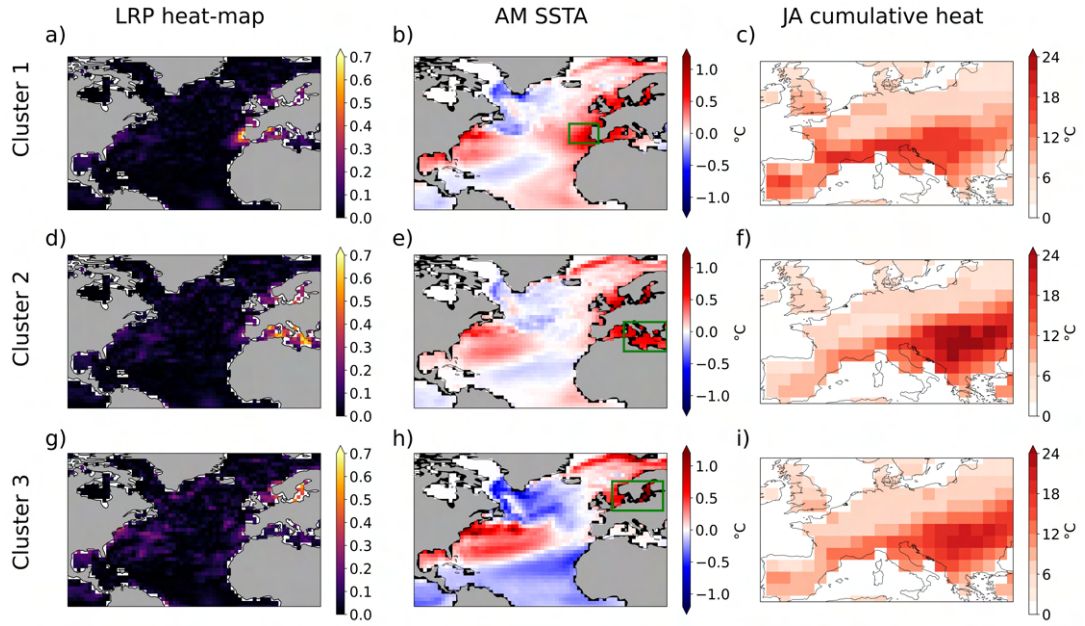


Figure B.3: K-means clustering of layerwise relevance propagation (LRP) heat-maps for correctly classified European summer heatwave years with model confidence above 60%. Cluster composites of; (a, d, g) LRP heat-maps; (b, e, h) April and May mean SSTAs; (c, f, i) July and August heatwave intensity expressed as cumulative heat. Cluster one contains 1,103 samples, cluster two 814 samples and cluster three 903 samples.

In addition to the North Atlantic pattern, we find that positive and negative SSTAs surrounding the European continent also precede EuSHW years and non-EuSHW years (Figures B.2a and B.2c). The LRP heat-map composites of correctly classified samples highlight the European regional seas as the most important regions to differentiate EuSHW and non-EuSHW years (Figures B.2b and B.2d). We hypothesize that the heat-maps of correctly classified EuSHW years contain distinct patterns that highlight different regional SSTAs, and that different regional SSTAs are the precursor of different EuSHWs.

We obtain three LRP clusters all showing the tripolar North Atlantic pattern with consistent positive SSTAs in the Subtropical Gyre (Figures B.3b, B.3e and B.3h), but highlighting different regional seas (Figures B.3a, B.3d and B.3g). The first cluster highlights positive SSTAs west of the Iberian Peninsula and contains the strongest western EuSHWs (Figures B.3a–B.3c). The second cluster highlights positive SSTAs in the Mediterranean Sea and contains the strongest southeastern EuSHWs (Figures B.3d–B.3f). The third cluster highlights positive SSTAs in the North Sea and the Baltic Sea, and contains southeastern EuSHWs, although of less intensity than cluster 2 (Figures B.3g–B.3i).

Our results suggest that, on the one hand, the tripolar North Atlantic pattern with negative SSTAs in SPG and western tropical Atlantic and positive SSTAs in the Subtropical Gyre is a precursor of EuSHWs, in agreement with Cassou et al. (2005), Duchez et al. (2016), and Wulff et al. (2017). However, the most consistent feature within the tripolar North Atlantic pattern preceding EuSHWs is the anomalously warm Subtropical Gyre. Disturbances in Subtropical North Atlantic SSTs and the respective diabatic heating anomalies are thought to be a source of Rossby waves

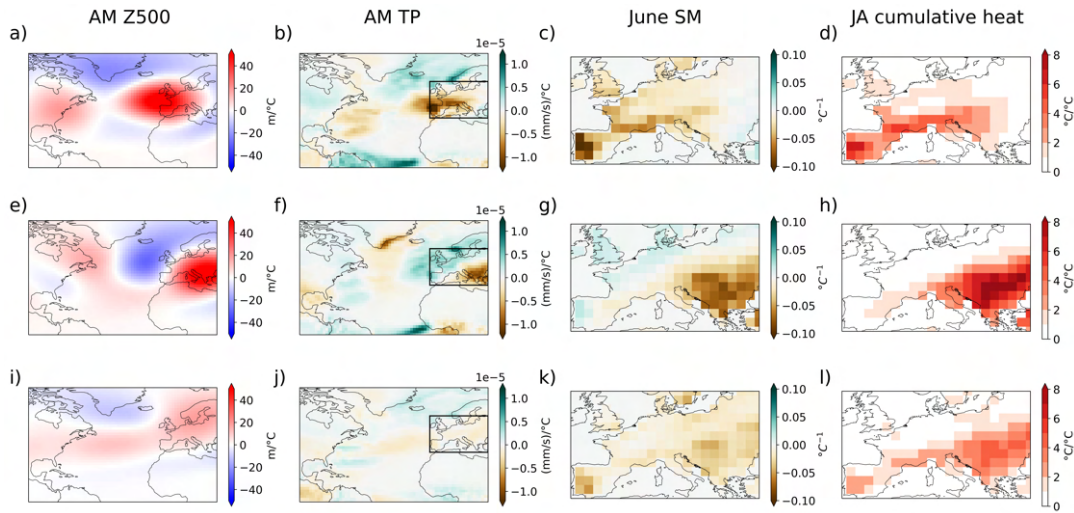


Figure B.4: Linear regression coefficients for the entire historical MPI Grand-Ensemble data set between April and May (AM) mean sea surface temperature anomalies averaged over the boxes in Figures B.3b, B.3e and B.3h and; (a, e, i) AM mean Z500 anomalies; (b, f, j) AM mean total precipitation anomalies; (c, g, k) June soil moisture anomalies; (d, h, l) July and August heatwave intensity anomalies expressed as cumulative heat.

which affect the European climate (Chen et al., 2020; Li and Ruan, 2018; Lim, 2015). On the other hand, the regional seas highlighted by the LRP heat-maps as the most relevant precursors for EuSHWs, appear to be the precursors of different types of EuSHWs.

The tripolar North Atlantic pattern, forced by winter atmospheric circulation anomalies, persists through spring and creates a reversed ocean-to-atmosphere forcing, preconditioning the occurrence of EuSHWs (Czaja and Frankignoul, 2002; Gastineau and Frankignoul, 2015; Ossó et al., 2018; Rodwell, 2002). In addition, we argue that positive regional SSTAs enhance the persistence of distinct blocking patterns and modulate spring precipitations and early summer SM anomalies in different European regions, preconditioning different types of EuSHWs. Although the SM can have a memory of several months (Hagemann and Stacke, 2015) and negative anomalies could be the product of the preceding dry winter, the soil dries considerably from early spring to early summer, consistent with our explanation (Figure B.6 in Supplementary Information 5).

Using the complete historical MPI-GE data set we linearly regress AM SSTAs averaged over the regional seas (boxes in Figures B.3b, B.3e and B.3h) with AM Z500 anomalies, AM TP anomalies, June SM anomalies and JA cumulative heat anomalies on a grid-point level. Positive AM SSTAs west of the Iberian Peninsula relate to positive AM Z500 anomalies, dry AM TP and June SM anomalies, and an increase of EuSHW intensity in western Europe (Figures B.4a–B.4d). Positive AM SSTAs in the Mediterranean Sea relate to positive AM Z500 anomalies, dry AM TP and June SM anomalies, and an increase of EuSHW intensity in southeastern Europe (Figures B.4e–B.4h). Positive AM SSTAs in the North Sea and the Baltic Sea relate to positive AM Z500 anomalies, dry AM TP and June SM anomalies, and an increase of EuSHW intensity in southeastern Europe (Figures B.4i–B.4l).

The relationship between SSTAs in the North Sea and Baltic Sea and the intensity of southeastern EuSHWs (Figures B.4i–B.4l) could be a combined effect of regional SSTAs and the winter NAO. Unlike positive SSTAs west of the Iberian Peninsula and in the Mediterranean Sea, positive SSTAs in the North Sea and Baltic Sea are related to the tripolar North Atlantic pattern (Figure B.7 in Supplementary Information 5), which is an imprint of the winter NAO (Czaja and Frankignoul, 2002). During the positive phase of NAO, the storm-track is shifted northward warming the North Sea and the Baltic Sea, drying the SM in southern Europe due to negative precipitation anomalies, and preconditioning southern EuSHWs (Wanner et al., 2001). However, positive SSTAs in the North Sea can directly enhance the occurrence of EuSHWs by reducing the meridional temperature gradient and baroclinic activity, allowing the persistence of high pressure systems over Europe (Feudale and Shukla, 2011).

Feudale and Shukla (2007, 2011) related the North Sea and the Mediterranean Sea to the 2003 EuSHW, which impacted western Europe. The 2003 EuSHW had several other contributing factors, including the northward displacement of the Azores high which relates to a deficit of precipitation in western Europe (Garcia-Herrera et al., 2010; Rashid et al., 2012). The northward displacement of Azores high could have been responsible for the strong deficit of SM in western Europe, and hence, for the westward location of the 2003 EuSHW. We find that the positive SSTAs west of the Iberian Peninsula are a precursor of western EuSHWs, and positive SSTAs in the North Sea and Mediterranean Sea are a precursor of southeastern EuSHWs, in agreement with Ionita et al. (2017) who showed that the warm Mediterranean Sea relates to dry and hot summer conditions in eastern Europe.

From our analysis, we are unable to conclude whether regional SSTAs play an active or passive role in the development of EuSHWs. We propose that positive regional SSTAs act as a heatwave amplification factor enhancing the persistence of blocking in different European regions. However, it is plausible that several episodes of blocking increase the regional SSTAs while reducing the SM. Future model experiments are required to disentangle the role of regional seas.

Our findings are only based on the MPI-GE data set, which contains model biases (Giorgetta et al., 2013; Hagemann et al., 2013; Müller et al., 2018). It has been shown that model wind biases can alter the propagation of Rossby waves induced by North Atlantic SSTAs (Li et al., 2021), which are relevant for modulating the atmospheric state and triggering heatwaves (Cassou et al., 2005; Kornhuber et al., 2020; Wulff et al., 2017). Although it has been demonstrated that the low resolution version of the MPI model represents well the connection between spring North Atlantic SSTA and Eurasian surface temperatures via atmospheric wave trains (Chen et al., 2021), the availability of other large ensembles with high temporal frequency and spatial resolution would aid to verify our results.

4 CONCLUSIONS

We investigate spring North Atlantic SSTAs as a precursor of EuSHWs combining the historical MPI-GE data set with NN based explainable artificial intelligence method, LRP. We identify the tripolar North Atlantic pattern with negative SSTAs in the SPG and the western tropical Atlantic as a precursor of EuSHWs. The most con-

sistent feature of the tripolar pattern preceding EuSHWs is the positive SSTAs in the Subtropical Gyre. In addition, positive SSTAs in different regional seas emerge as the most robust precursors of different EuSHWs. While positive spring SSTAs west of the Iberian Peninsula precede western EuSHWs, positive spring SSTAs in the Mediterranean Sea, the North Sea and the Baltic Sea precede southeastern EuSHWs. The regional SSTAs can be related to distinct anticyclonic anomalies in spring, reducing the precipitation and leading to distinct patterns of negative SM anomalies in early summer. The patterns of SM anomalies resemble the location of the most intense EuSHWs. Here, we show that the combination of the spring tripolar North Atlantic pattern and regional SSTAs could aid in predicting the occurrence and location of EuSHWs.

ACKNOWLEDGMENTS

G.B.-A. is supported by the German Ministry of Education and Research (BMBF) under the ClimXtreme project NA2EE (Grant 01LP1902F). A.D. is supported by A4 (Aigéin, Aeráid, agus athrú Atlantaigh), funded by the Marine Institute (grant PBA/CC/18/01). E.A.B. is supported, in part, by the Regional and Global Model Analysis program area of the U.S. Department of Energy's Office of Biological and Environmental Research as part of the Program for Climate Model Diagnosis and Intercomparison project. We acknowledge the Deutsches Klimarechenzentrum (DKRZ) for the computational resources. We thank David Marcolino Nielsen for the insightful comments on the manuscript. We thank the two reviewers for their thoughtful comments.

DATA AVAILABILITY STATEMENT

Data used in this study are available on the following website after registering at World Data Centre for Climate (<http://hdl.handle.net/21.14106/5a1b88c2bb1ae7736779602e6a201a119b7cf1bc>).

The supporting material contains three additional figures. Figure B.5 shows that the performance of our NN model classifying non-EuSHW years and EuSHW years depends on the heatwave intensity expressed as cumulative heat. Our NN performs the best classifying non-EuSHW years with lowest cumulative heat (Fig. B.5a) and EuSHW years with highest cumulative heat (Fig. B.5b). Hence, the composites of correctly classified samples mainly contain years with lowest and highest heatwave intensity. Above 88% of non-EuSHW years with lowest cumulative heat and above 94% of EuSHW years with highest cumulative heat are correctly classified. In contrast, the performance is lowest for non-EuSHW years with highest cumulative heat (Fig. B.5a) and for EuSHW years with lowest cumulative heat (Fig. B.5b). Above 62% of non-EuSHW years with highest cumulative heat and above 57% of EuSHW years with lowest cumulative heat are correctly classified. We train 100 NN models with randomly shuffled training and validation sets, and compute the uncertainties with 90% confidence of validation set performance.

Figure B.6 shows January to June soil moisture anomaly composites of correctly classified EuSHW years. Negative soil moisture anomalies are detected in winter in southern Europe (Fig. B.6a,b). From March to June the soil moisture considerably dries and the negative anomalies extend northward (Fig. B.6c-f).

Figure B.7 shows the correlation between April and May SSTAs in the Subtropical Gyre and April and May SSTAs in the North Atlantic. SSTAs in the Subtropical Gyre are related to the tripolar North Atlantic pattern and weakly related to the North Sea and Baltic Sea SSTAs. In contrast, SSTAs in the Subtropical Gyre are not related to SSTAs west of Iberian Peninsula and in the eastern Mediterranean Sea. This supports our result that the phase of the spring tripolar North Atlantic pattern and positive spring SSTAs in regional seas provide different information regarding the upcoming EuSHWs.

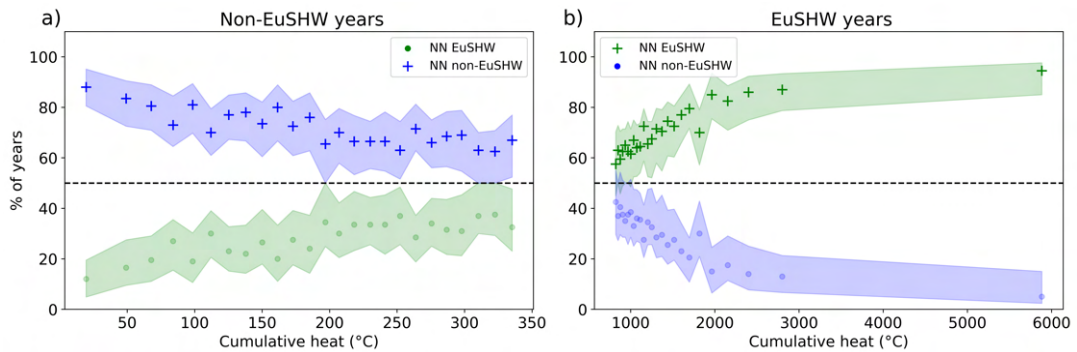


Figure B.5: The percentage of years that the NN classifies as EuSHW (green) and non-EuSHW (blue). The years are binned in groups of 200 samples depending on their heatwave intensity expressed as cumulative heat; **(a)** non-EuSHW years; **(b)** EuSHW years. Crosses indicate the correctly classified cases. The dashed line in 50% indicate the probability of classifying each category by chance. Shading represents the uncertainty of training/validating split. The uncertainty is computed with 90% confidence of validation set performance after training 100 NN models.

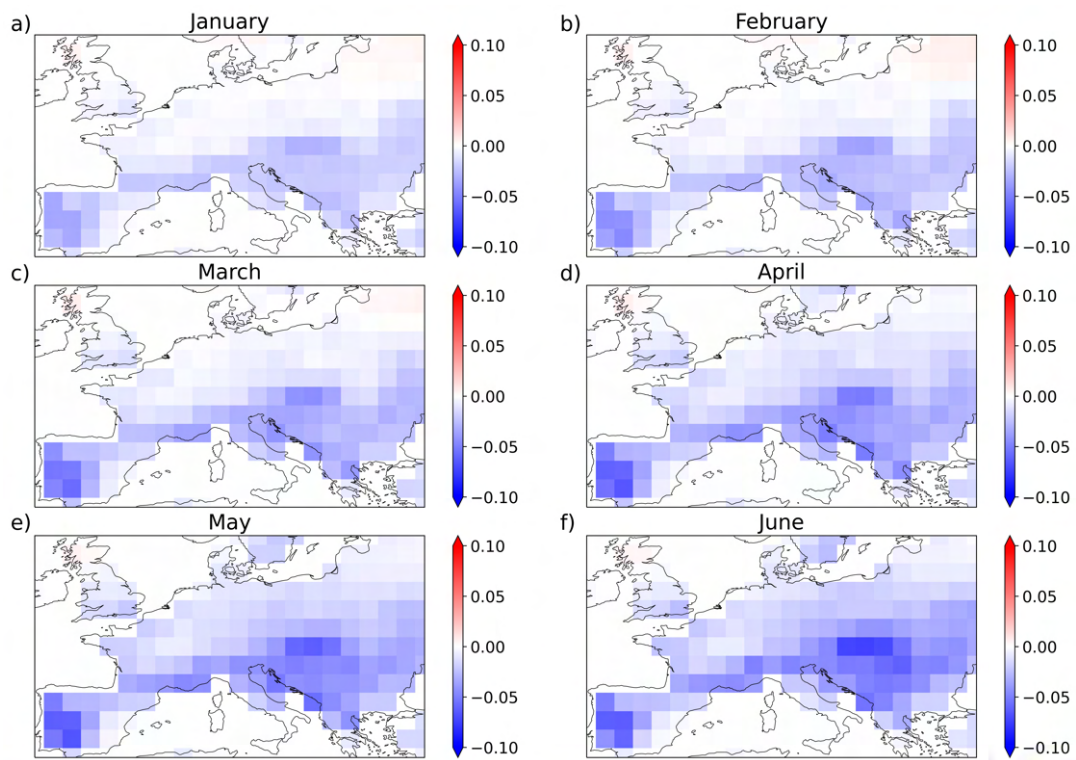


Figure B.6: Soil moisture anomaly composite of correctly classified EuSHW years during; (a) January; (b) February; (c) March; (d) April; (e) May; (f) June.

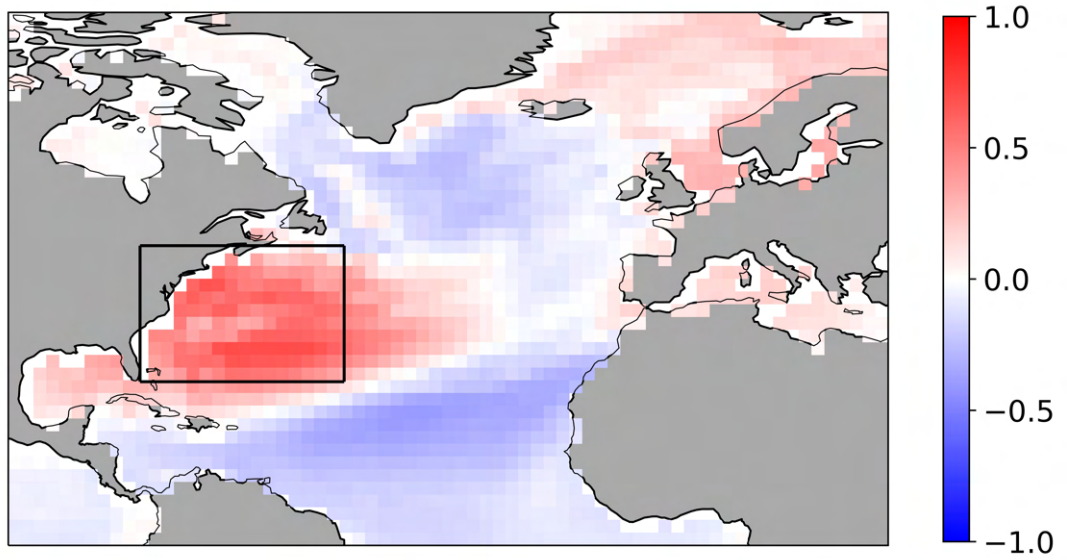


Figure B.7: Grid-point correlation between April and May SSTAs averaged over the Subtropical Gyre (black box; 80°W-50°W, 25°N-45°N) and April and May North Atlantic SSTAs.

ON THE APPLICABILITY OF SPRING NORTH ATLANTIC SEA
SURFACE TEMPERATURES AS AN INDICATOR OF EUROPEAN
SUMMER HEATWAVES

The work in this appendix is intended to be submitted as:

Beobide-Arsuaga, G., Düsterhus, A., Müller, W. A., and Baehr, J. (2023). "On the applicability of spring North Atlantic sea surface temperatures as an indicator of European summer heatwaves" - *to be submitted*.

The contribution to this paper is as follows: G.B.-A. conceived and designed the study, performed the analysis and wrote the paper. A.D., W.A.M. and J.B. contributed through discussions and reviewed the manuscript.

On the applicability of spring North Atlantic sea surface temperatures as an indicator of European summer heatwaves

Goratz Beobide-Arsuaga^{1,2}, André Düsterhus³, Wolfgang A. Müller⁴, and Johanna Baehr¹,

¹Institute of Oceanography, Center for Earth System Research and Sustainability (CEN), Universität Hamburg, Hamburg, Germany

²International Max Planck Research School on Earth System Modelling, Max Planck Institute for Meteorology, Hamburg, Germany

³Maynooth University, ICARUS, Department of Geography, Maynooth, Ireland

⁴Max Planck Institute for Meteorology, Ocean in the Earth System, Hamburg, Germany

- To be submitted -

ABSTRACT

Past case studies have shown that different spring and early summer North Atlantic sea surface temperature anomaly (SSTA) patterns influenced the occurrence of recent European summer heatwaves (EuSHWs). Yet, the low number of observed events has restricted the identification of the most relevant North Atlantic SSTAs to anticipate EuSHWs. A recent model-based study proposed that the phase of spring North Atlantic tripolar pattern (NATP) indicates the occurrence of EuSHWs, and that spring SSTAs in different regional seas indicate the location of EuSHWs. Here, we combine ERA5 reanalysis product, EOBS and OISST observational datasets, and the GFCS2.1 seasonal forecast system to investigate the applicability of spring NATP and regional seas as an indicator of EuSHW occurrence. We find that all datasets agree on an increased western EuSHW probability with the positive phase of spring NATP, and on an increased southeastern EuSHW probability with positive SSTAs in the Mediterranean or in the North and Baltic Seas. Additionally, the probability of EuSHW occurrence is reduced for negative SSTAs averaged over the regional seas. Our results indicate that spring North Atlantic SSTAs are applicable to anticipate EuSHWs and could be used to develop early warning systems.

1 INTRODUCTION

The intensity, frequency, and duration of heatwaves have increased globally since the 1950s (Perkins-Kirkpatrick and Lewis, 2020). In Europe in particular, the intensity of heatwaves has incremented four times when compared to the rest of the northern midlatitudes and caused severe ecosystem, human and economic losses

(Bastos et al., 2020; D'Ippoliti et al., 2010; García-León et al., 2021; Rousi et al., 2022). Yet, our ability to anticipate European summer heatwaves (EuSHWs) remains very limited. The accurate prediction of EuSHW, such as the onset, duration, and intensity, can hardly be achieved beyond a few weeks before their occurrence (Lavaysse et al., 2019; Pyrina and Domeisen, 2022). However, slow-varying boundary conditions precondition the development of EuSHWs and could be useful indicators of EuSHW occurrence (Domeisen et al., 2023; Quesada et al., 2012).

Persistent spring North Atlantic sea surface temperature anomalies (SSTAs) have been associated with the stationary position of the jet stream, which allows long-lasting blocking anticyclones to maintain over Europe, reduce the precipitations and the moisture of the soil, and modulate the occurrence and intensity of recent EuSHWs (Fischer et al., 2007; Gastineau and Frankignoul, 2015; Ossó et al., 2020; Saeed et al., 2014). On the one hand, the negative SSTAs in the Subpolar Gyre and in the tropical Atlantic, both part of the positive phase of the North Atlantic tripolar pattern (NATP), have been associated with the occurrence of the 2015 EuSHW (Duchez et al., 2016; Wulff et al., 2017). Additionally, the positive phase of the NATP also preceded the 2018 EuSHW which affected a large part of Northern Europe (Rousi et al., 2023). On the other hand, positive SSTAs in the North Sea and Mediterranean Sea have been associated with the 2003 EuSHW (Feudale and Shukla, 2007, 2011). Due to the large variety of physical processes associated with a limited number of observed events, the relevance of the North Atlantic SSTAs to anticipate EuSHWs remains inconclusive.

Beobide-Arsuaga et al. (2023), based on a single-model large-ensemble historical run, proposed that the phase of the spring NATP indicates the occurrence of EuSHWs. In addition, the study argues that positive spring SSTAs in different regional seas enhance the persistence of the blocking anticyclones and reduce precipitation and soil moisture in different European regions, indicating the occurrence of different EuSHWs. While positive SSTAs around the Iberian Peninsula indicate the occurrence of western EuSHWs, positive SSTAs in the Mediterranean, North, and Baltic Seas indicate the occurrence of southeastern EuSHWs. Here, we combine ERA5 reanalysis product and EOBS and OISST observational datasets with GFCS2.1 seasonal forecast system to test the applicability of spring NATP and regional SSTAs as an indicator of EuSHW occurrence.

2 DATA AND METHODS

This study employs ERA5 reanalysis product, EOBS and OISST observational datasets, and the GFCS2.1 seasonal forecast system for the period 1982-2022 (Cornes et al., 2018; Fröhlich et al., 2021; Hersbach et al., 2020; Huang et al., 2021). GFCS2.1 consists of 30 ensemble members initialized in May, it has been operational since 2020, and it is based on the MPI high-resolution model (Müller et al., 2018). The ensemble members use the assimilation run at the end of April as initial conditions. The assimilation run is a separate simulation that continuously nudges the atmospheric and oceanic reanalysis data to bring the model's state close to the observed state of the climate system (Fröhlich et al., 2021). All datasets have been linearly interpolated to the regular Gaussian grid of the GFCS2.1 with a horizontal resolution of approximately 100km.

We use July and August daily maximum surface temperatures (T_{2max}) over Europe ($10^{\circ}W-30^{\circ}E$, $35^{\circ}N-60^{\circ}N$), and April and May (AM hereafter) mean sea surface temperature anomalies (SSTAs) relative to the 1982-2011 reference period over the North Atlantic ($100^{\circ}W-30^{\circ}E$, $0^{\circ}-80^{\circ}N$). For the GFCS2.1 SSTAs, we combine April from the assimilation run and May from individual ensemble members.

We identify heatwaves with a percentile-based definition (Perkins and Alexander, 2013). A heatwave day is considered for each land grid-point when T_{2max} exceeds the 90th percentile based on a centered 15-day running window and 1982-2011 reference period for at least three consecutive days. We use the cumulative heat metric to calculate the intensity of heatwaves (Perkins-Kirkpatrick and Lewis, 2020). The metric integrates the difference between T_{2max} and the percentile-based threshold during heatwave days. We weight the cumulative heat of each grid-point by the cosine of the latitude and obtain one map per year expressing the intensity of heatwaves consistent with Beobide-Arsuaga et al. (2023).

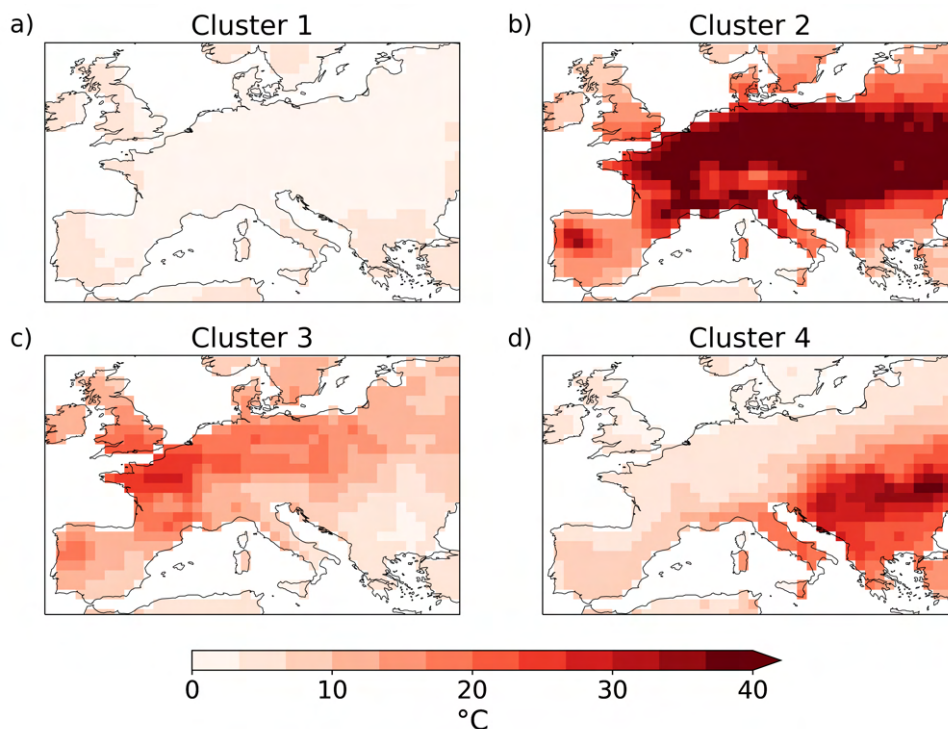


Figure C.1: K-means composite means of July and August cumulative heat for; **(a)** cluster one with 936 non-EuSHW years; **(b)** cluster two with 42 most intense EuSHWs; **(c)** cluster three with 189 western EuSHWs; **(d)** cluster four with 145 southeastern EuSHWs.

We differentiate the strongest heatwave years from the weakest heatwave years using a K-means model (Hartigan and Wong, 1979). Four clusters are obtained after fitting the model with the heatwave intensity maps from ERA5, EOBS, and GFCS2.1 (Fig. C.1). The first cluster contains 936 years with the weakest heatwave intensity. We refer to them as non-EuSHW years. The other three clusters show heatwaves of distinct spatial patterns and we refer to them as EuSHW years. Cluster two contains 42 EuSHW years that affect a large part of the European domain, from which only two belong to ERA5 and EOBS. Because of the reduced number of years, we do

not do any analysis restricted only to cluster two. Cluster three contains 189 years that affect western Europe and we refer to them as western EuSHWs years. Cluster four contains 145 years that affect southeastern Europe and we refer to them as southeastern EuSHW years. The proportion of cluster members is very similar in all datasets: 63.5%, 2.4%, 19.5% and 14.6% for ERA5, 65.9%, 2.4%, 19.5% and 12.2% for EOBS, and 71.7%, 3.3%, 14.1% and 10.9% for GFCS2.1.

We test if the occurrence of EuSHWs is favored by specific AM North Atlantic SSTAs. Following Beobide-Arsuaga et al. (2023), we focus on the phase of the NATP (80°W-60°W, 25°N-35°N minus 40°W-25°W, 45°N-55°N) and on the regional seas (REG): around the Iberian Peninsula (IB; 12°W-5°E, 33°N-47°N), the Mediterranean Sea (MED; 5°E-28°E, 30°N-45°N), and the North and Baltic Seas (NS; 3°W-28°E, 50°N-65°N). We select 30% most extreme AM SSTA cases averaged over the areas of interest. We refer to the highest and lowest 30% cases as positive and negative cases, respectively (e.g. +NATP refers to the years of 30% highest NATP values, and -NATP refers to the years of 30% lowest NATP values). We compute the probability of EuSHW occurrence for each selected subset and divide it with the probability of EuSHW occurrence during the entire study period. The positive or negative AM SSTAs are related to an increase in EuSHW occurrence if the probability ratio is above one. The uncertainties are computed with a 90% confidence after bootstrapping over each SSTA subset. The results are insensitive to the selection of different SSTA percentage cases.

3 RESULTS

ERA5 AM SSTA composites suggest that a positive NATP and positive regional SSTAs, and a negative NATP and negative regional SSTAs precede EuSHW years and non-EuSHW years, respectively (Fig. C.2). The composites with observational datasets show indistinct results (not shown). The composite for EuSHW years shows the NATP with positive SSTAs in the Subtropical Gyre and negative anomalies in the Subpolar Gyre and the tropical Atlantic, and positive SSTAs in the regional seas (Fig. C.2a). The composite for non-EuSHW years shows the NATP with negative SSTAs in the Subtropical Gyre and positive anomalies in the Subpolar Gyre and the tropical Atlantic, and negative SSTAs in the regional seas (Fig. C.2b).

We find that the occurrence of EuSHWs is related to the positive phase of the NATP and to the positive regional SSTAs (Fig. C.2c). In ERA5 the probability ratio is 1.47 and 1.26 when selecting the positive NATP or REG cases, respectively. In observational datasets the probability ratio is 1.58 for positive NATP and REG cases. In contrast, the probability ratio of EuSHW occurrence in ERA5 and observational datasets is 0.42 and 0.45 for negative REG cases, indicating that the probability of EuSHW occurrence is reduced when AM SSTAs averaged over the regional seas are negative. The occurrence of EuSHWs for negative NATP cases is close to climatology, with probability ratios of 0.84 and 0.90 in ERA5 and observational datasets, and hence, the occurrence of EuSHWs is not related to the negative phase of NATP.

However, not all EuSHWs are more likely to occur when the NATP is in the positive phase (Fig. C.3). While the probability ratio of western EuSHWs is 2.37 for positive NATP cases (Fig. C.3a), the probability ratio of southeastern EuSHWs is practically zero (Fig. C.3b). In addition, western and southeastern EuSHWs are

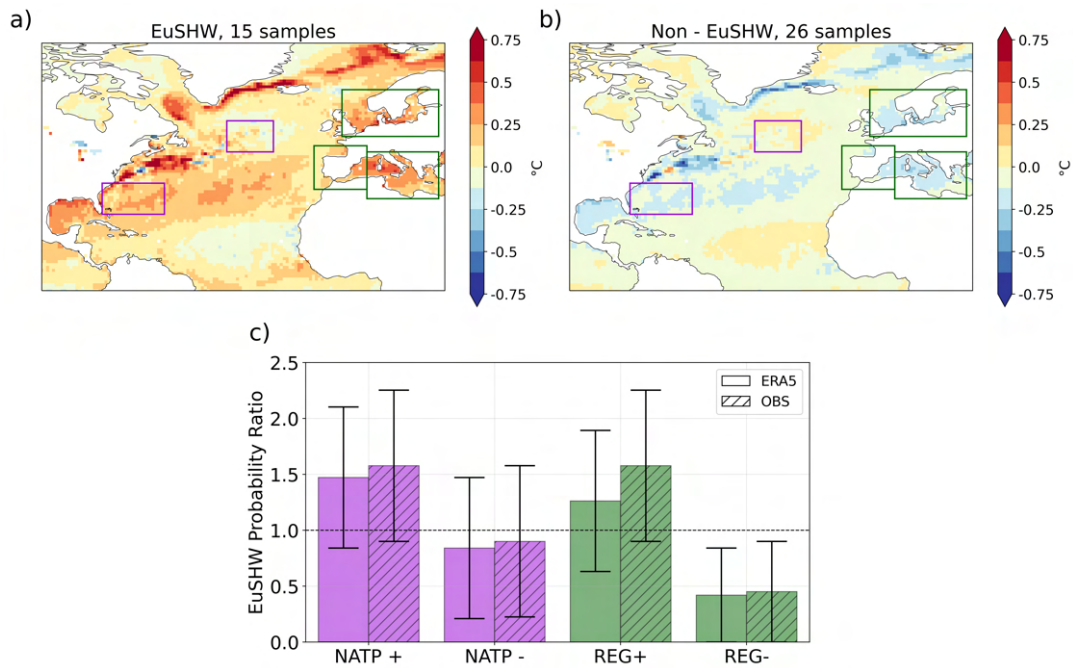


Figure C.2: ERA5 April and May mean SSTA composites relative to the mean for; **(a)** European summer heatwave years (EuSHW); **(b)** non European summer heatwave years (non-EuSHW). **(c)** The probability of EuSHW occurrence relative to the whole study period for the upper (+) and lower (-) 30th percentile of the North Atlantic tripolar pattern (NATP) index and regional SSTAs (REG) in ERA5 and observational datasets (OBS). The NATP index is computed as the SSTA difference between the southern and northern averaged lilac boxes in (a) and (b). REG is computed as the SSTA mean over the three green boxes in (a) and (b). The uncertainties are computed with a 90% confidence after bootstrapping over each SSTA subset.

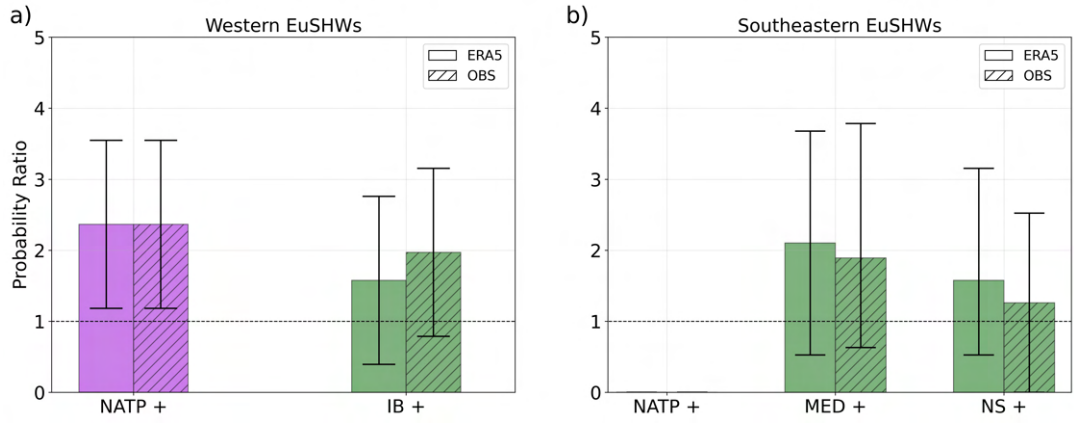


Figure C.3: For ERA5 and observational datasets (OBS); **(a)** The probability of western European summer heatwave (EuSHW) occurrence relative to the climatology for the upper 30th percentile of the North Atlantic tripolar pattern (NATP) index and the SSTAs surrounding the Iberian Peninsula (IB); **(b)** The probability of southeastern EuSHW occurrence relative to the climatology for the upper 30th percentile of the NATP index, and the SSTAs in the Mediterranean Sea (MED) and in the North and Baltic Seas (NS). The NATP index is computed as the SSTA difference between the southern and northern averaged lilac boxes in Fig. C.2a,b. IB, MED and NS are computed as the averaged SSTAs over the green boxes in Fig. C.2a,b. The uncertainties are computed with a 90% confidence after bootstrapping over each SSTA subset.

related to SSTAs in different regional seas. Western EuSHWs are related to positive IB cases, although the relationship is not as strong as for positive NATP cases (Fig. C.3a). The probability ratio of western EuSHWs for positive IB cases is 1.58 and 1.97 in ERA5 and observational datasets. In contrast, southeastern EuSHWs are mainly related to positive SSTAs in the Mediterranean Sea. The probability ratio for positive MED cases is 2.1 and 1.89 in ERA5 and observational datasets. Southeastern EuSHWs are also, albeit less, related to positive SSTAs in the North and Baltic Seas with a probability ratio of 1.58 and 1.26 in ERA5 and observational datasets.

GFCs2.1 AM SSTA composites for EuSHWs and non-EuSHWs are very similar to the ones obtained with ERA5. The composite for EuSHW years shows a positive phase of NATP and positive SSTAs in the regional seas (Fig. C.4a). The composite for non-EuSHWs years shows a negative phase of NATP and negative SSTAs in the regional (Fig. C.4b).

However, unlike in ERA5 and observational datasets, we find that in the GFCs2.1 the occurrence of EuSHWs is significantly more related to positive SSTAs averaged over the regional seas than to the positive phase of NATP (Fig. C.4c). The probability ratio of EuSHWs is 1.75 for positive REG cases and 1.35 for positive NATP cases. Furthermore, the occurrence of EuSHWs is significantly less likely for the years with negative SSTAs averaged over the regional seas than for the years with the negative phase of NATP. The probability ratios are 0.11 and 0.41 for negative REG and negative NATP cases, respectively. These differences indicate that the development of EuSHWs in GFCs2.1 is more sensitive to the SSTAs in the regional seas than to the NATP.

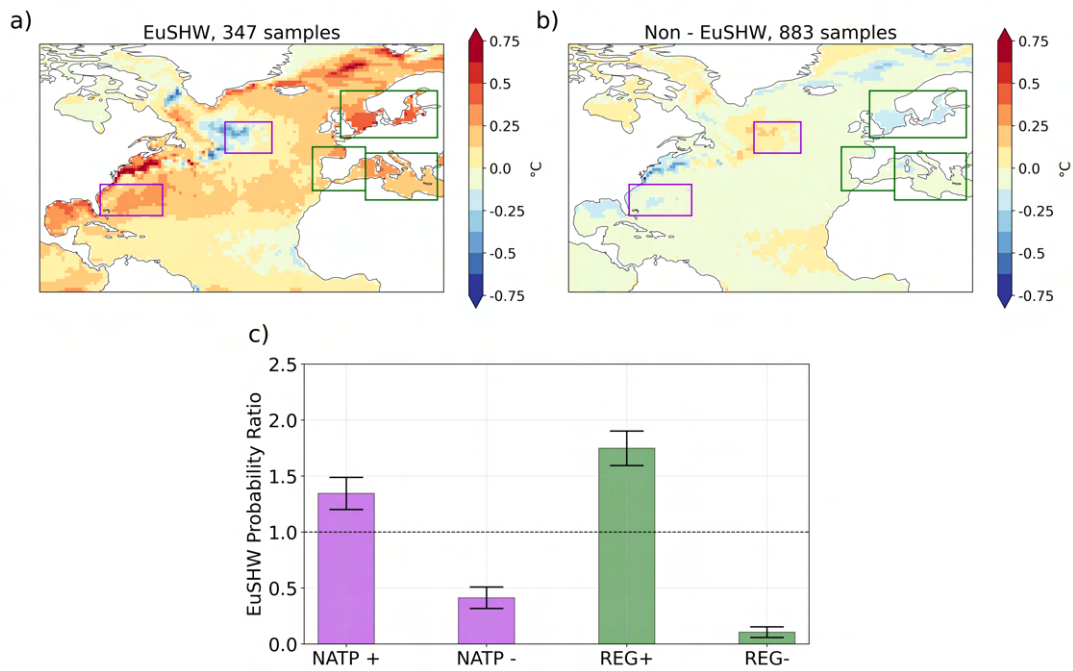


Figure C.4: GFCS2.1 April and May mean SSTA composites relative to the mean for; **(a)** European summer heatwave years (EuSHW); **(b)** non European summer heatwave years (non-EuSHW). **(c)** The probability of EuSHW occurrence relative to the climatology for the upper (+) and lower (-) 30th percentile of the North Atlantic tripolar pattern (NATP) index and regional SSTAs (REG) in ERA5 and EOBS. The NATP index is computed as the SSTA difference between the southern and northern averaged lilac boxes in (a) and (b). REG is computed as the SSTA mean over the three green boxes in (a) and (b). The uncertainties are computed with a 90% confidence after bootstrapping over each SSTA subset.

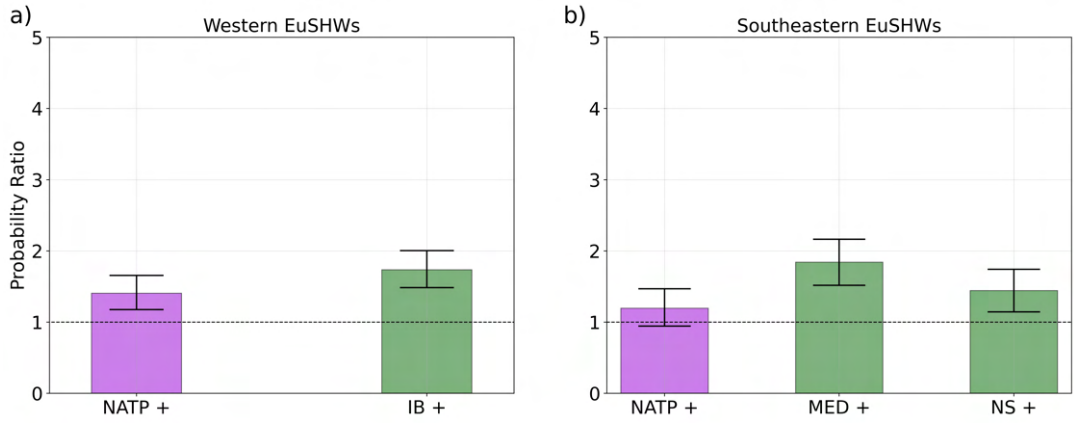


Figure C.5: For GFCs2.1; **(a)** The probability of western European summer heatwave (EuSHW) occurrence relative to the climatology for the upper 30th percentile of the North Atlantic tripolar pattern (NATP) index and the SSTAs surrounding the Iberian Peninsula (IB); **(b)** The probability of southeastern EuSHW occurrence relative to the climatology for the upper 30th percentile of the NATP index, and the SSTAs in the Mediterranean Sea (MED) and in the North and Baltic Seas (NS). The NATP index is computed as the SSTA difference between the southern and northern averaged lilac boxes in Fig. C.4a,b. IB, MED and NS are computed as the averaged SSTAs over the green boxes in Fig. C.4a,b. The uncertainties are computed with a 90% confidence after bootstrapping over each SSTA subset.

A stronger relationship to positive regional SSTAs than to positive NATP is consistent for both western and southeastern EuSHWs (Fig. C.5). In disagreement with ERA5 and observational datasets, western EuSHWs are more related to positive SSTAs surrounding the Iberian Peninsula than to the positive phase of NATP (Fig. C.5a). The probability ratio of western EuSHWs for positive IB cases is 1.73 and for positive NATP cases is 1.41. Similarly, western EuSHWs are more related to positive SSTAs in the Mediterranean Sea and in the North and Baltic Seas than to the positive phase of NATP (Fig. C.5b). The probability ratio of southeastern EuSHWs is 1.84, 1.44, and 1.19 for positive MED, NS, and NATP cases, respectively.

4 DISCUSSION

ERA5 and the observational datasets have large uncertainties due to the reduced number of samples. Although we find that the positive phase of NATP robustly relates to the occurrence of western EuSHWs and not to the southeastern EuSHWs, the relationship between both types of EuSHWs and the SSTAs in different regional seas is not as clear. The uncertainty of the probability ratio with 90% confidence does not cross the value one when relating western and southeastern EuSHWs to the positive NATP. But the uncertainty of the probability ratio with 90% confidence goes below one when relating western and southeastern EuSHWs to positive SSTAs in different regional seas.

In our analysis we find some differences between ERA5 and observational datasets which also highlight the limitation of the sample size. We see the main differences when relating EuSHWs in general, and western and southeastern EuSHWs in par-

ticular to the SSTAs in the regional seas. On the one hand, the differences partly emerge from the intensity of EuSHWs. Our K-mean model identifies the year 2021 as a southeastern EuSHW in ERA5, but it identifies as non-EuSHW in EOBS. On the other hand, the differences also emerge from AM regional SSTAs, where small differences between the datasets can affect the probability ratio. Nevertheless, the results are qualitatively the same for ERA5 and observational datasets.

In contrast, GFCS2.1 with 30 members per year provides a larger sample size and therefore has smaller uncertainties. In GFCS2.1 we find a robust relationship between the regional SSTAs and EuSHWs in agreement with previous studies (Beobide-Arsuaga et al., 2023; Feudale and Shukla, 2007, 2011). The range of the probability ratio uncertainty does not cross the value one when relating western and southeastern EuSHWs to the positive IB cases, and to the positive MED and NS cases, respectively.

However, GFCS2.1 might represent spurious relationships between AM North Atlantic SSTAs and EuSHWs. Unlike in ERA5 and observational datasets, we find that in GFCS2.1 the western EuSHWs are more related to the SSTAs around the Iberian Peninsula than to the positive phase of NATP. The model also disagrees by showing that southeastern EuSHWs are related to the positive phase of NATP. This implies that the GFCS2.1 simulates false western and southeastern EuSHWs when the SSTAs around the Iberian Peninsula are positive and when the phase of the NATP is positive, respectively.

The results from GFCS2.1 are in closer agreement with Beobide-Arsuaga et al. (2023), who use the low-resolution uninitialized MPI historical simulations than with ERA5 and observational datasets, than to the results from ERA5 and observational datasets, and it hints towards unrealistic physical connections of the MPI climate model (Müller et al., 2018). The disagreement suggests that the influence of the NATP on the European summer climate is misrepresented by some ensemble members, in agreement with Neddermann et al. (2019). The seasonal predictability of EuSHWs could be improved by sub-selecting the ensemble members that capture the physical connection between the NATP and EuSHWs (Dobrynin et al., 2018; Neddermann et al., 2019).

Nevertheless, we do find overlapping results between GFCS2.1, and ERA5 and observational datasets reinforcing that spring North Atlantic SSTAs are applicable to anticipate EuSHWs. All datasets indicate that the probability of EuSHW occurrence is low when the SSTAs averaged over the regional seas are negative. All datasets agree that the probability of western EuSWH occurrence is higher when the NATP is positive. They also agree that the probability of southeastern EuSHW occurrence is higher when the SSTAs in the Mediterranean Sea or in the North and Baltic Seas are positive.

5 CONCLUSIONS

In the present study, we investigate the applicability of spring North Atlantic SSTAs as an indicator of EuSHW occurrence. Based on Beobide-Arsuaga et al. (2023), we test if the NATP and regional SSTAs are related to the occurrence of EuSHWs using ERA5 reanalysis data, EOBS and OISST observational datasets, and the GFCS2.1 seasonal forecast system. All datasets agree that the probability of western EuSHWs

is increased during the positive phase of NATP and that the probability of southeastern EuSHWs is increased when the SSTAs in the Mediterranean Sea or in the North and Baltic Seas are positive. We also find that the probability of EuSHW occurrence is reduced when the SSTAs averaged over the regional seas are negative. However, unlike in ERA5 and observational datasets, in GFCS2.1 the occurrence of western EuSHWs is more related to the positive SSTAs around the Iberian Peninsula than to the positive NATP. In addition, in GFCS2.1 the positive NATP also relates to the occurrence of southeastern EuSHWs, which is not the case in the observational datasets. Overall, we demonstrate that certain spring North Atlantic SSTAs are robust precursors of EuSHWs, and thus, might be used to develop early warning systems.

ACKNOWLEDGMENTS

G.B.-A. is supported by the German Ministry of Education and Research (BMBF) under the ClimXtreme project NA2EE (Grant 01LP1902F). A.D. is supported by A4 (Aigéin, Aeráid, agus athrú Atlantaigh), funded by the Marine Institute (grant PBA/CC/18/01). We acknowledge the Deutsches Klimarechenzentrum (DKRZ) for the computational resources.

BIBLIOGRAPHY

- Aleman, S., Beltran, J., Perez, A., & Ganzfried, S. (2019). Predicting hurricane trajectories using a recurrent neural network. *Proceedings of the AAAI Conference on Artificial Intelligence*, 33(01), 468–475. <https://doi.org/10.1609/aaai.v33i01.3301468>
- Añel, J. A., Fernández-González, M., Labandeira, X., López-Otero, X., & de la Torre, L. (2017). Impact of cold waves and heat waves on the energy production sector. *Atmosphere*, 8(11), 1–13. <https://doi.org/10.3390/atmos8110209>
- Austin, J. F. (1980). The blocking of middle latitude westerly winds by planetary waves. *Quarterly Journal of the Royal Meteorological Society*, 106(448), 327–350. <https://doi.org/10.1002/qj.49710644807>
- Bach, S., Binder, A., Montavon, G., Klauschen, F., Müller, K. R., & Samek, W. (2015). On pixel-wise explanations for non-linear classifier decisions by layer-wise relevance propagation. *PLoS ONE*, 10(7), 1–46. <https://doi.org/10.1371/journal.pone.0130140>
- Barriopedro, D., García-Herrera, R., Ordóñez, C., Miralles, D. G., & Salcedo-Sanz, S. (2023). Heat Waves: Physical Understanding and Scientific Challenges. *Reviews of Geophysics*, 61(2). <https://doi.org/10.1029/2022rg000780>
- Bastos, A., Ciais, P., Friedlingstein, P., Sitch, S., Pongratz, J., Fan, L., Wigneron, J. P., Weber, U., Reichstein, M., Fu, Z., Anthoni, P., Arneth, A., Haverd, V., Jain, A. K., Joetzjer, E., Knauer, J., Lienert, S., Loughran, T., McGuire, P. C., ... Zaehle, S. (2020). Direct and seasonal legacy effects of the 2018 heat wave and drought on European ecosystem productivity. *Science Advances*, 6(24), 1–14. <https://doi.org/10.1126/sciadv.aba2724>
- Beobide-Arsuaga, G. (2023). European summer heatwave catalogue. DOKU at DKRZ. https://www.wdc-climate.de/ui/entry?acronym=DKRZ%7B%5C_%7DLTA%7B%5C_%7D1075%7B%5C_%7Dds00028
- Beobide-Arsuaga, G., Düsterhus, A., Müller, W. A., Barnes, E. A., & Baehr, J. (2023). Spring Regional Sea Surface Temperatures as a Precursor of European Summer Heatwaves. *Geophysical Research Letters*, 50(2), 1–8. <https://doi.org/10.1029/2022GL100727>
- Bjerknes, J. (1964). Atlantic Air-Sea Interaction. *Advances in Geophysics*, 10, 1–82. [https://doi.org/10.1016/S0065-2687\(08\)60005-9](https://doi.org/10.1016/S0065-2687(08)60005-9)
- Błazejczyk, K., Jendritzky, G., Bröde, P., Fiala, D., Havenith, G., Epstein, Y., Psikuta, A., & Kampmann, B. (2013). An introduction to the Universal thermal climate index (UTCI). *Geographia Polonica*, 86(1), 5–10. <https://doi.org/10.7163/GPol.2013.1>
- Brás, T. A., Seixas, J., Carvalhais, N., & Jagermeyr, J. (2021). Severity of drought and heatwave crop losses tripled over the last five decades in Europe. *Environmental Research Letters*, 16(6). <https://doi.org/10.1088/1748-9326/abf004>
- Cassou, C., Terray, L., & Phillips, A. S. (2005). Tropical Atlantic influence on European heat waves. *Journal of Climate*, 18(15), 2805–2811. <https://doi.org/10.1175/JCLI3506.1>

- Chen, S., Wu, R., & Chen, W. (2021). Influence of North Atlantic sea surface temperature anomalies on springtime surface air temperature variation over Eurasia in CMIP5 models. *Climate Dynamics*, 57(9-10), 2669–2686. <https://doi.org/10.1007/s00382-021-05826-5>
- Chen, S., Wu, R., Chen, W., Hu, K., & Yu, B. (2020). Structure and dynamics of a springtime atmospheric wave train over the North Atlantic and Eurasia. *Climate Dynamics*, 54(11-12), 5111–5126. <https://doi.org/10.1007/s00382-020-05274-7>
- Cornes, R. C., van der Schrier, G., van den Besselaar, E. J., & Jones, P. D. (2018). An Ensemble Version of the E-OBS Temperature and Precipitation Data Sets. *Journal of Geophysical Research: Atmospheres*, 123(17), 9391–9409. <https://doi.org/10.1029/2017JD028200>
- Czaja, A., & Frankignoul, C. (1999). Influence of the North Atlantic SST on the atmospheric circulation. *Geophysical Research Letters*, 26(19), 2969–2972.
- Czaja, A., & Frankignoul, C. (2002). Observed Impact of Atlantic SST Anomalies on the North Atlantic Oscillation. *Journal of Climate*, 15(18), 2707–2712. [https://doi.org/10.1175/1520-0442\(2002\)015<2707:OTRONA>2.0.CO;2](https://doi.org/10.1175/1520-0442(2002)015<2707:OTRONA>2.0.CO;2)
- Della-Marta, P. M., Luterbacher, J., von Weissenfluh, H., Xoplaki, E., Brunet, M., & Wanner, H. (2007). Summer heat waves over western Europe 1880-2003, their relationship to large-scale forcings and predictability. *Climate Dynamics*, 29(2-3), 251–275. <https://doi.org/10.1007/s00382-007-0233-1>
- de Oliveira, M. M., Ebecken, N. F. F., de Oliveira, J. L. F., & de Azevedo Santos, I. (2009). Neural network model to predict a storm surge. *Journal of Applied Meteorology and Climatology*, 48(1), 143–155. <https://doi.org/10.1175/2008JAMC1907.1>
- D’Ippoliti, D., Michelozzi, P., Marino, C., De’Donato, F., Menne, B., Katsouyanni, K., Kirchmayer, U., Analitis, A., Medina-Ramón, M., Paldy, A., Atkinson, R., Kovats, S., Bisanti, L., Schneider, A., Lefranc, A., Iñiguez, C., & Perucci, C. A. (2010). The impact of heat waves on mortality in 9 European cities: Results from the EuroHEAT project. *Environmental Health: A Global Access Science Source*, 9(1), 1–9. <https://doi.org/10.1186/1476-069X-9-37>
- Dobrynin, M., Domeisen, D. I., Müller, W. A., Bell, L., Brune, S., Bunzel, F., Düsterhus, A., Fröhlich, K., Pohlmann, H., & Baehr, J. (2018). Improved Teleconnection-Based Dynamical Seasonal Predictions of Boreal Winter. *Geophysical Research Letters*, 45(8), 3605–3614. <https://doi.org/10.1002/2018GL077209>
- Domeisen, D. I., Eltahir, E. A., Fischer, E. M., Knutti, R., Perkins-Kirkpatrick, S. E., Schär, C., Seneviratne, S. I., Weisheimer, A., & Wernli, H. (2023). Prediction and projection of heatwaves. *Nature Reviews Earth and Environment*, 4(1), 36–50. <https://doi.org/10.1038/s43017-022-00371-z>
- Dongare, A., Kharde, R., & Kachare, A. (2012). Introduction to Artificial Neural Network (ANN) Methods. *International Journal of Engineering and Innovative Technology (IJEIT)*, 2(1), 189–194. <https://citeseerx.ist.psu.edu/viewdoc/download?doi=10.1.1.1082.1323%7B%5C&%7Drep=rep1%7B%5C&%7Dtype=pdf>
- Duchez, A., Frajka-Williams, E., Josey, S. A., Evans, D., Grist, J. P., Marsh, R., McCarthy, G. D., Sinha, B., Berry, D. I., & Hirschi, J. (2016). Drivers of exceptionally cold North Atlantic Ocean temperatures and their link to the 2015

- European heat wave. *Environmental Research Letters*, 11(7). <https://doi.org/10.1088/1748-9326/11/7/074004>
- Easterling, D. R., Horton, B., Jones, P. D., Peterson, T. C., Karl, T. R., Parker, D. E., Salinger, M. J., Razuvayev, V., Plummer, N., Jamason, P., & Folland, C. K. (1997). Maximum and minimum temperature trends for the globe. *Science*, 277(5324), 364–367. <https://doi.org/10.1126/science.277.5324.364>
- Feudale, L., & Shukla, J. (2007). Role of Mediterranean SST in enhancing the European heat wave of summer 2003. *Geophysical Research Letters*, 34(3), 2–5. <https://doi.org/10.1029/2006GL027991>
- Feudale, L., & Shukla, J. (2011). Influence of sea surface temperature on the European heat wave of 2003 summer. Part II: a modeling study. *Climate Dynamics*, 36(9-10), 1705–1715. <https://doi.org/10.1007/s00382-010-0789-z>
- Fischer, E. M., & Schär, C. (2010). Consistent geographical patterns of changes in high-impact European heatwaves. *Nature Geoscience*, 3(6), 398–403. <https://doi.org/10.1038/ngeo866>
- Fischer, E. M., Seneviratne, S. I., Vidale, P. L., Lüthi, D., & Schär, C. (2007). Soil moisture-atmosphere interactions during the 2003 European summer heat wave. *Journal of Climate*, 20(20), 5081–5099. <https://doi.org/10.1175/JCLI4288.1>
- Fröhlich, K., Dobrynin, M., Isensee, K., Gessner, C., Paxian, A., Pohlmann, H., Haak, H., Brune, S., Früh, B., & Baehr, J. (2021). The German Climate Forecast System: GCFS. *Journal of Advances in Modeling Earth Systems*, 13(2). <https://doi.org/10.1029/2020MS002101>
- García-Herrera, R., Díaz, J., Trigo, R. M., Luterbacher, J., & Fischer, E. M. (2010). A review of the European summer heat wave of 2003. *Critical Reviews in Environmental Science and Technology*, 40(4), 267–306. <https://doi.org/10.1080/10643380802238137>
- García-León, D., Casanueva, A., Standardi, G., Burgstall, A., Flouris, A. D., & Nybo, L. (2021). Current and projected regional economic impacts of heatwaves in Europe. *Nature Communications*, 12(1), 1–10. <https://doi.org/10.1038/s41467-021-26050-z>
- Gastineau, G., & Frankignoul, C. (2015). Influence of the North Atlantic SST variability on the atmospheric circulation during the twentieth century. *Journal of Climate*, 28(4), 1396–1416. <https://doi.org/10.1175/JCLI-D-14-00424.1>
- Giorgetta, M. A., Jungclaus, J., Reick, C. H., Legutke, S., Bader, J., Böttinger, M., Brovkin, V., Crueger, T., Esch, M., Fieg, K., Glushak, K., Gayler, V., Haak, H., Hollweg, H. D., Ilyina, T., Kinne, S., Kornbluh, L., Matei, D., Mauritsen, T., ... Stevens, B. (2013). Climate and carbon cycle changes from 1850 to 2100 in MPI-ESM simulations for the Coupled Model Intercomparison Project phase 5. *Journal of Advances in Modeling Earth Systems*, 5(3), 572–597. <https://doi.org/10.1002/jame.20038>
- Hagemann, S., Loew, A., & Andersson, A. (2013). Combined evaluation of MPI-ESM land surface water and energy fluxes. *Journal of Advances in Modeling Earth Systems*, 5(2), 259–286. <https://doi.org/10.1029/2012MS000173>
- Hagemann, S., & Stacke, T. (2015). Impact of the soil hydrology scheme on simulated soil moisture memory. *Climate Dynamics*, 44(7-8), 1731–1750. <https://doi.org/10.1007/s00382-014-2221-6>

- Hartigan, J. A., & Wong, M. A. (1979). A K-Means Clustering Algorithm. *Journal of the Royal Statistical Society: Series C (Applied Statistics)*, 28(1), 100–108.
- Hersbach, H., Bell, B., Berrisford, P., Hirahara, S., Horányi, A., Muñoz-Sabater, J., Nicolas, J., Peubey, C., Radu, R., Schepers, D., Simmons, A., Soci, C., Abdalla, S., Abellan, X., Balsamo, G., Bechtold, P., Biavati, G., Bidlot, J., Bonavita, M., ... Thépaut, J. N. (2020). The ERA5 global reanalysis. *Quarterly Journal of the Royal Meteorological Society*, 146(730), 1999–2049. <https://doi.org/10.1002/qj.3803>
- Huang, B., Liu, C., Banzon, V., Freeman, E., Graham, G., Hankins, B., Smith, T., & Zhang, H. M. (2021). Improvements of the Daily Optimum Interpolation Sea Surface Temperature (DOISST) Version 2.1. *Journal of Climate*, 34(8), 2923–2939. <https://doi.org/10.1175/JCLI-D-20-0166.1>
- Ionita, M., Tallaksen, L. M., Kingston, D. G., Stagge, J. H., Laaha, G., Van Lanen, H. A., Scholz, P., Chelcea, S. M., & Haslinger, K. (2017). The European 2015 drought from a climatological perspective. *Hydrology and Earth System Sciences*, 21(3), 1397–1419. <https://doi.org/10.5194/hess-21-1397-2017>
- IPCC. (2021). Climate change 2021: The physical science basis. In V. Masson-Delmotte, P. Zhai, A. Pirani, S. L. Connors, C. Péan, S. Berger, et al. (Eds.) *Contribution of working group I to the sixth assessment report of the intergovernmental panel on climate change*, 2.
- IPCC. (2023). Climate Change 2023: Synthesis Report. *A Report of the Intergovernmental Panel on Climate Change. Contribution of Working Groups I, II and III to the Sixth Assessment Report of the Intergovernmental Panel on Climate Change [Core Writing Team, H. Lee and J. Romero (eds.)]. IPCC, Geneva, Switzer.*
- Katz, R. W., & Brown, B. G. (1992). Extreme events in a changing climate: variability is more important than averages. *Climatic change*, 21(3), 289–302. <https://doi.org/10.1007/BF00139728>
- Kneller, L. (2023). *Determining a seasonal connection between Arctic Spring Sea Ice and European Summer Heatwaves using machine learning methods* (Bachelor thesis, available at the Universität Hamburg library). Universität Hamburg.
- Kornhuber, K., Coumou, D., Vogel, E., Lesk, C., Donges, J. F., Lehmann, J., & Horton, R. M. (2020). Amplified Rossby waves enhance risk of concurrent heatwaves in major breadbasket regions. *Nature Climate Change*, 10(1), 48–53. <https://doi.org/10.1038/s41558-019-0637-z>
- Lavaysse, C., Naumann, G., Alfieri, L., Salamon, P., & Vogt, J. (2019). Predictability of the European heat and cold waves. *Climate Dynamics*, 52(3-4), 2481–2495. <https://doi.org/10.1007/s00382-018-4273-5>
- Lecun, Y., Bengio, Y., & Hinton, G. (2015). Deep learning. *Nature*, 521(7553), 436–444. <https://doi.org/10.1038/nature14539>
- Li, J., & Ruan, C. (2018). The North Atlantic-Eurasian teleconnection in summer and its effects on Eurasian climates. *Environmental Research Letters*, 13(2). <https://doi.org/10.1088/1748-9326/aa9d33>
- Li, R. K. K., Tam, C. Y., Lau, N. C., Sohn, S., Ahn, J. B., & O'Reilly, C. (2021). Forcing mechanism of the Silk Road pattern and the sensitivity of Rossby-wave source hotspots to mean-state winds. *Quarterly Journal of the Royal Meteorological Society*, 147(737), 2533–2546. <https://doi.org/10.1002/qj.4039>

- Lim, Y. K. (2015). The East Atlantic/West Russia (EA/WR) teleconnection in the North Atlantic: climate impact and relation to Rossby wave propagation. *Climate Dynamics*, 44(11-12), 3211–3222. <https://doi.org/10.1007/s00382-014-2381-4>
- Lorenz, E. N. (1963). Deterministic nonperiodic flow. *Journal of atmospheric sciences*, 20(2), 130–141.
- Lowe, D., Ebi, K. L., & Forsberg, B. (2011). Heatwave early warning systems and adaptation advice to reduce human health consequences of heatwaves. *International Journal of Environmental Research and Public Health*, 8(12), 4623–4648. <https://doi.org/10.3390/ijerph8124623>
- Maher, N., Milinski, S., Suarez-Gutierrez, L., Botzet, M., Dobrynin, M., Kornblueh, L., Kröger, J., Takano, Y., Ghosh, R., Hedemann, C., Li, C., Li, H., Manzini, E., Notz, D., Putrasahan, D., Boysen, L., Claussen, M., Ilyina, T., Olonscheck, D., ... Marotzke, J. (2019). The Max Planck Institute Grand Ensemble: Enabling the Exploration of Climate System Variability. *Journal of Advances in Modeling Earth Systems*, 11(7), 2050–2069. <https://doi.org/10.1029/2019MS001639>
- Maher, N., Milinski, S., & Ludwig, R. (2021). Large ensemble climate model simulations: Introduction, overview, and future prospects for utilising multiple types of large ensemble. *Earth System Dynamics*, 12(2), 401–418. <https://doi.org/10.5194/esd-12-401-2021>
- Marzban, C., & Witt, A. (2001). A Bayesian neural network for severe-hail size prediction. *Weather and Forecasting*, 16(5), 600–610. [https://doi.org/10.1175/1520-0434\(2001\)016<0600:ABNNFS>2.0.CO;2](https://doi.org/10.1175/1520-0434(2001)016<0600:ABNNFS>2.0.CO;2)
- Mayer, K. J., & Barnes, E. A. (2021). Subseasonal Forecasts of Opportunity Identified by an Explainable Neural Network. *Geophysical Research Letters*, 48(10), 1–9. <https://doi.org/10.1029/2020GL092092>
- Mearns, L. O., Katz, R. W., & Schneider, S. H. (1984). Extreme High-Temperature Events: Changes in their Probabilities with Changes in Mean Temperature. *Journal of Applied Meteorology and Climatology*, 23(12), 1601–1613.
- Mecking, J. V., Drijfhout, S. S., Hirschi, J. J., & Blaker, A. T. (2019). Ocean and atmosphere influence on the 2015 European heatwave. *Environmental Research Letters*, 14(11). <https://doi.org/10.1088/1748-9326/ab4d33>
- Meehl, G. A., Arblaster, J. M., & Branstator, G. (2012). Mechanisms contributing to the warming hole and the consequent U.S. East-west differential of heat extremes. *Journal of Climate*, 25(18), 6394–6408. <https://doi.org/10.1175/JCLI-D-11-00655.1>
- Merz, B., Kuhlicke, C., Kunz, M., Pittore, M., Babeyko, A., Bresch, D. N., Domeisen, D. I., Feser, F., Koszalka, I., Kreibich, H., Pantillon, F., Parolai, S., Pinto, J. G., Punge, H. J., Rivalta, E., Schröter, K., Strehlow, K., Weisse, R., & Wurpts, A. (2020). Impact Forecasting to Support Emergency Management of Natural Hazards. *Reviews of Geophysics*, 58(4), 1–52. <https://doi.org/10.1029/2020RG000704>
- Montavon, G., Lapuschkin, S., Binder, A., Samek, W., & Müller, K. R. (2017). Explaining nonlinear classification decisions with deep Taylor decomposition. *Pattern Recognition*, 65(May 2016), 211–222. <https://doi.org/10.1016/j.patcog.2016.11.008>

- Müller, W. A., Jungclaus, J. H., Mauritsen, T., Baehr, J., Bittner, M., Budich, R., Bunzel, F., Esch, M., Ghosh, R., Haak, H., Ilyina, T., Kleine, T., Kornblüeh, L., Li, H., Modali, K., Notz, D., Pohlmann, H., Roeckner, E., Stemmler, I., ... Marotzke, J. (2018). A Higher-resolution Version of the Max Planck Institute Earth System Model (MPI-ESM1.2-HR). *Journal of Advances in Modeling Earth Systems*, 10(7), 1383–1413. <https://doi.org/10.1029/2017MS001217>
- Neddermann, N. C., Müller, W. A., Dobrynin, M., Düsterhus, A., & Baehr, J. (2019). Seasonal predictability of European summer climate re-assessed. *Climate Dynamics*, 53(5-6), 3039–3056. <https://doi.org/10.1007/s00382-019-04678-4>
- Ossó, A., Sutton, R., Shaffrey, L., & Dong, B. (2018). Observational evidence of European summer weather patterns predictable from spring. *Proceedings of the National Academy of Sciences of the United States of America*, 115(1), 59–63. <https://doi.org/10.1073/pnas.1713146114>
- Ossó, A., Sutton, R., Shaffrey, L., & Dong, B. (2020). Development, Amplification, and Decay of Atlantic/European Summer Weather Patterns Linked to Spring North Atlantic Sea Surface Temperatures. *Journal of Climate*, 33(14), 5939–5951. <https://doi.org/10.1175/JCLI-D-19-0613.1>
- Patterson, M. (2023). North-West Europe Hottest Days Are Warming Twice as Fast as Mean Summer Days. *Geophysical Research Letters*, 50(10), 1–10. <https://doi.org/10.1029/2023GL102757>
- Perkins, S. E., & Alexander, L. V. (2013). On the measurement of heat waves. *Journal of Climate*, 26(13), 4500–4517. <https://doi.org/10.1175/JCLI-D-12-00383.1>
- Perkins-Kirkpatrick, S. E., & Lewis, S. C. (2020). Increasing trends in regional heatwaves. *Nature Communications*, 11(1), 1–8. <https://doi.org/10.1038/s41467-020-16970-7>
- Prodhomme, C., Materia, S., Ardilouze, C., White, R. H., Batté, L., Guemas, V., Fragkoulidis, G., & García-Serrano, J. (2021). Seasonal prediction of European summer heatwaves. *Climate Dynamics*, (0123456789). <https://doi.org/10.1007/s00382-021-05828-3>
- Pyrina, M., & Domeisen, D. I. (2022). Subseasonal predictability of onset, duration, and intensity of European heat extremes. *Quarterly Journal of the Royal Meteorological Society*, 149(750), 84–101. <https://doi.org/10.1002/qj.4394>
- Quesada, B., Vautard, R., Yiou, P., Hirschi, M., & Seneviratne, S. I. (2012). Asymmetric European summer heat predictability from wet and dry southern winters and springs. *Nature Climate Change*, 2(10), 736–741. <https://doi.org/10.1038/nclimate1536>
- Rashid, S. A., Iqbal, M. J., & Hussain, M. A. (2012). Impact of North-South Shift of Azores High on Summer Precipitation over North West Europe. *International Journal of Geosciences*, 03(05), 992–999. <https://doi.org/10.4236/ijg.2012.325099>
- Rex, D. F. (1950). Blocking Action in the Middle Troposphere and its Effect upon Regional Climate. *Tellus*, 2(4), 275–301. <https://doi.org/10.3402/tellusa.v2i4.8603>
- Robine, J. M., Cheung, S. L. K., Le Roy, S., Van Oyen, H., Griffiths, C., Michel, J. P., & Herrmann, F. R. (2008). Death toll exceeded 70,000 in Europe during the summer of 2003. *Comptes Rendus - Biologies*, 331(2), 171–178. <https://doi.org/10.1016/j.crvi.2007.12.001>

- Rodwell, M. J. (2002). Atlantic air-sea interaction revisited. *International Geophysics*, 83(100), 185–197. [https://doi.org/10.1016/S0074-6142\(02\)80167-X](https://doi.org/10.1016/S0074-6142(02)80167-X)
- Rousi, E., Fink, A. H., Andersen, L. S., Becker, F. N., Beobide-Arsuaga, G., Breil, M., Cozzi, G., Heinke, J., Jach, L., Niermann, D., Petrovic, D., Richling, A., Riebold, J., Steidl, S., Suarez-Gutierrez, L., Tradowsky, J. S., Coumou, D., Düsterhus, A., Ellsäßer, F., ... Xoplaki, E. (2023). The extremely hot and dry 2018 summer in central and northern Europe from a multi-faceted weather and climate perspective. *Natural Hazards and Earth System Sciences*, 23(5), 1699–1718. <https://doi.org/10.5194/nhess-23-1699-2023>
- Rousi, E., Kornhuber, K., Beobide-Arsuaga, G., Luo, F., & Coumou, D. (2022). Accelerated western European heatwave trends linked to more-persistent double jets over Eurasia. *Nature Communications*, 13(1), 1–11. <https://doi.org/10.1038/s41467-022-31432-y>
- Saeed, S., Van Lipzig, N., Müller, W. A., Saeed, F., & Zanchettin, D. (2014). Influence of the circumglobal wave-train on European summer precipitation. *Climate Dynamics*, 43(1-2), 503–515. <https://doi.org/10.1007/s00382-013-1871-0>
- Samek, W., Montavon, G., Lapuschkin, S., Anders, C. J., & Müller, K. R. (2021). Explaining Deep Neural Networks and Beyond: A Review of Methods and Applications. *Proceedings of the IEEE*, 109(3), 247–278. <https://doi.org/10.1109/JPROC.2021.3060483>
- Seneviratne, S. I., Lüthi, D., Litschi, M., & Schär, C. (2006). Land-atmosphere coupling and climate change in Europe. *Nature*, 443(7108), 205–209. <https://doi.org/10.1038/nature05095>
- Song, Y., & Chen, H. (2023). Influence of the Late-Winter North Atlantic Tripole Sea Surface Temperature Anomalies on Spring Land Surface Temperature in Mid-to-High Latitudes of Western Eurasia. *Journal of Climate*, 36(15), 4933–4950. <https://doi.org/10.1175/jcli-d-22-0846.1>
- Stefanon, M., Dandrea, F., & Drobinski, P. (2012). Heatwave classification over Europe and the Mediterranean region. *Environmental Research Letters*, 7(1). <https://doi.org/10.1088/1748-9326/7/1/014023>
- Suarez-Gutierrez, L., Li, C., Müller, W. A., & Marotzke, J. (2018). Internal variability in European summer temperatures at 1.5 °C and 2 °C of global warming. *Environmental Research Letters*, 13(6). <https://doi.org/10.1088/1748-9326/aaba58>
- Toms, B. A., Barnes, E. A., & Ebert-Uphoff, I. (2020). Physically Interpretable Neural Networks for the Geosciences: Applications to Earth System Variability. *Journal of Advances in Modeling Earth Systems*, 12(9), 1–20. <https://doi.org/10.1029/2019MS002002>
- Toms, B. A., Barnes, E. A., & Hurrell, J. W. (2021). Assessing Decadal Predictability in an Earth-System Model Using Explainable Neural Networks. *Geophysical Research Letters*, 48(12). <https://doi.org/10.1029/2021GL093842>
- Treidl, R. A., Birch, E. C., & Sajecki, P. (1981). Blocking action in the northern hemisphere: A climatological study. *Atmosphere - Ocean*, 19(1), 1–23. <https://doi.org/10.1080/07055900.1981.9649096>
- Vogel, M. M., Zscheischler, J., Fischer, E. M., & Seneviratne, S. (2020). Development of future heatwaves for different hazard thresholds. *Journal of Geophysical Research: Atmospheres*. <https://doi.org/10.1029/2019jd032070>

- Wanner, H., Brönnimann, S., Casty, C., Gyalistras, D., Luterbacher, J., Schmutz, C., Stephenson, D. B., & Xoplaki, E. (2001). North atlantic oscillation—concepts and studies. *Surveys in geophysics*, 22, 321–381.
- Watanabe, M., & Kimoto, M. (2000). Atmosphere-ocean thermal coupling in the North Atlantic: A positive feedback. *Quarterly Journal of the Royal Meteorological Society*, 126(570), 3343–3369. <https://doi.org/10.1256/smsqj.57016>
- Weiland, R. S., van der Wiel, K., Selten, F., & Coumou, D. (2021). Intransitive atmosphere dynamics leading to persistent hot-dry or cold-wet European summers. *Journal of Climate*, 34(15), 6303–6317. <https://doi.org/10.1175/JCLI-D-20-0943.1>
- WMO. (1992). International meteorological vocabulary. 182 (2nd ed.)
- Wulff, C. ., Greatbatch, R. J., Domeisen, D., Gollan, G., & Hansen, F. (2017). Tropical Forcing of the Summer East Atlantic Pattern. *Geophysical Research Letters*, 44(21), 11, 166–11, 173. <https://doi.org/10.1002/2017GL075493>

DECLARATION

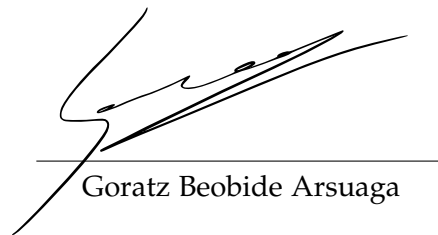
Eidesstattliche Versicherung

Declaration on Oath

Hiermit erkläre ich an Eides statt, dass ich die vorliegende Dissertationsschrift selbst verfasst und keine anderen als die angegebenen Quellen und Hilfsmittel benutzt habe.

I hereby declare upon oath that I have written the present dissertation independently and have not used further resources and aids than those stated.

Hamburg, den 26.07.2023



Goratz Beobide Arsuaga

